

UNCLASSIFIED



Australian Government
Department of Defence
Defence Science and
Technology Organisation

Analysis of Multilayered Printed Circuit Boards using Computed Tomography

Samuel Fox and Greg Perry

Cyber and Electronic Warfare Division
Defence Science and Technology Organisation

DSTO-TR-2973

ABSTRACT

Computed Tomography is a technique that can be performed using a set of X-ray images to re-create a three dimensional dataset which contains information about internal structure. Analysis of multilayered Printed Circuit Boards with their components using this technique allows for the non destructive evaluation of internal layers of failed boards. This report presents the results of computerised tomography on multilayered Printed Circuit Boards using a SkyScan 1076.

RELEASE LIMITATION

Approved for public release

UNCLASSIFIED

UNCLASSIFIED

Published by

*Cyber and Electronic Warfare Division
DSTO Defence Science and Technology Organisation
PO Box 1500
Edinburgh South Australia 5111 Australia*

*Telephone: 1300 333 362
Fax: (08) 7389 6567*

*© Commonwealth of Australia 2014
AR-015-962
May 2014*

APPROVED FOR PUBLIC RELEASE

UNCLASSIFIED

Analysis of Multilayered Printed Circuit Boards using Computed Tomography

Executive Summary

Multilayered Printed Circuit Boards (PCB) dominate most of the electronic equipment in use today. The multilayered architecture has allowed the top and bottom surfaces of the PCB to be used primarily for component mounting with the majority of tracks on the internal layers. The complexity of the PCB depends on the fabrication process with some manufacturers producing PCBs with up to 35 layers. Feature size has also been reduced, with signal tracks approaching 25 μm wide and vias small enough to be completely obscured by even the smallest of surface mount components. This has led to more compact, densely populated complex PCBs that present a challenge for any testing or fault analysis.

Set-to-work testing and fault analysis of any electronic circuit require access to various circuit elements and signal lines. Traditional methods such as visual inspection and mechanical probing are not practical for complex multilayered PCBs due to the number of internal signal lines that cannot be accessed from the outside. 2D X-ray imaging can assist but this manual approach is time consuming due to the number of internal conductors that may need to be analysed.

X-ray Computed Tomography (CT) is primarily used in medical imaging but has been shown to be effective as a fault analysis tool in the PCB and semiconductor industry. The X-ray source rotates around the object producing a dataset of 2D X-ray slices. This dataset can then be reconstructed into a full three dimensional (3D) image of the object including any internal layers of a PCB.

In this report we describe examples of the use of a SkyScan 1076 X-ray CT system as a non-destructive tool to analyse a number of PCBs. The experiments focused on investigating the main parameters affecting the 3D reconstructed images as well as advantages and disadvantages of using a CT system over a conventional X-ray system.

It was found that once the parameter settings have been set correctly for the particular sample a complete dataset could be obtained automatically. This allowed the collection of high resolution PCB datasets to be scanned overnight then reconstructed the following day. Furthermore, multiple datasets could be acquired using a batch scan to allow different regions to be scanned with the same settings. This minimises the amount of time the operator needs to run similar scans on the same sample, but requires reconfiguration of the detector when the X-ray settings have been changed. This is important since densely populated areas on the PCB required longer X-ray exposure times than sparse areas to obtain the same level of detail.

UNCLASSIFIED

The raw dataset could also be processed multiple times and using different processing software including those designed for materials analysis. This level of analysis is not available using standard X-ray systems and allows not only internal faults on multilayered PCBs to be identified but more importantly may aid in determining the cause of the fault. However, the large datasets from the higher resolution scans could not be processed using a standard PC and required a high end graphics processor. Generally, the smaller the internal tracks and the more internal layers the higher the resolution needed and the larger the datasets.

X-ray imaging of PCBs in general has its own set of problems including image artifacts from X-raying metal objects, change in penetration depth affecting the contrast and shading from dense components blurring other materials. This can corrupt the raw datasets and degrade the reconstructed images. Internal ground and voltage planes in some of the samples were not easily observable and appeared as a lightly shaded area on the PCB. Adjusting the frame averaging and X-ray source filtering helped to better resolve these hard to observe features including smaller internal tracks. Furthermore, increasing the resolution of the CT systems will reduce some image artifacts but will proportionally increase the dataset. This can be problematic when scanning larger PCBs.

Although the maximum PCB size for the SkyScan 1076 was 65 mm x 400 mm the range of samples used allowed a thorough assessment of the issues involved in using CT to conduct fault analysis on complex multilayered PCBs. The assessment has highlighted the importance and the time taken to correctly process the datasets to obtain suitable reconstructed 3D images. It has also shown the advantages and disadvantages between CT and real time X-ray imaging.

The perfect system where a 3D image optimised for a particular multilayered PCB is automatically produced is still far from reality. However, the use of CT for materials analysis and fault recognition is gaining momentum in the PCB and semiconductor industry. This has led to improvements in post processing algorithms and reconstruction software and this trend is expected to continue.

UNCLASSIFIED

UNCLASSIFIED

Authors

Samuel Fox

Cyber and Electronic Warfare Division

Samuel Fox was first employed by the Electronic Warfare and Radar Division in December 2010. He is currently in Electro-Optic Countermeasures Group. Samuel works on embedded system design and software optimisation of complex electro-optical systems, including the set to work and characterisation of these systems. He has a Bachelor of Engineering (Electrical and Electronic) from the University of Adelaide.

Greg Perry

Cyber and Electronic Warfare Division

Greg Perry was first employed by the Electronic Warfare and Radar Division (EWRD) in April 1994. He worked as a technical officer setting to work and testing electronics for EW systems until 2000 when he moved to Japan to live. From 2000 until 2003 Greg worked for Kodan Electronics designing and setting-to-work electronic circuits for marine and underground radar systems. In 2004 he worked as a technical translator translating technical documentation from Japanese to English. Greg moved back to Australia in 2005 and worked as a contractor in EWRD for Electro-Optic Technologies (EOT) group. He was re-employed by EWRD in December 2005 and is currently in Electro-Optic Countermeasures Group (EOCM). Greg manages a laboratory focused on testing and analysis of complex electro-optic systems. He has a degree in Physics (Optics and Photonics) from the University of Adelaide and an Associate Diploma in Electronic Engineering from University of South Australia.

UNCLASSIFIED

UNCLASSIFIED

This page is intentionally blank

UNCLASSIFIED

Contents

1. INTRODUCTION.....	1
2. EXPERIMENT	2
2.1 Experiment Objectives.....	2
2.2 Equipment Used.....	2
2.2.1 SkyScan 1076 micro-CT.....	2
2.2.2 Nrecon Reconstruction Software.....	3
2.2.3 Analysis Software.....	3
2.2.4 PCB Samples	4
2.3 SkyScan 1076 Configuration.....	4
2.3.1 Contrast.....	4
2.3.2 Resolution.....	5
2.3.3 Dynamic Colour Range	6
2.3.4 Metal Artifacts	7
2.4 Cross-section Reconstruction Configuration	8
2.4.1 Software Artifact Reduction.....	8
2.4.2 Computational Power.....	8
2.5 2D Cross-section Results	9
2.5.1 Board Warp and Flatness	9
2.5.2 Continuity	10
2.6 3D Reconstruction Model Results.....	11
2.6.1 Volume Rendering.....	11
2.6.2 Attenuation Rendering.....	13
2.6.3 Maximum Intensity Projection.....	13
3. CONCLUSIONS	15
4. ACKNOWLEDGEMENTS	18
5. REFERENCES	18
APPENDIX A: X-RAY PHYSICS.....	19
A.1. Artifact Summary	19
A.1.1 Appearances of Image Artifacts	19
A.1.2 System Design Artifacts	21
A.1.3 Sample Based Artifacts	23
A.2. Definitions	25
A.2.1 X-Ray Spectrum	25

APPENDIX B:	SKYSCAN 1076 TECHNICAL SPECIFICATIONS	27
B.1.	Equipment Limitations	27
B.2.	Software Limitations	28
B.3.	Setup Procedure.....	28
B.3.1	<i>Start Up</i>	28
B.3.2	<i>Sample Preparation</i>	28
B.3.3	<i>X-ray Setup</i>	29
B.3.4	<i>Scan Setup</i>	30
B.4.	Experiment Configuration	31
B.5.	Reconstruction Algorithm Comparison	32
APPENDIX C:	CALCULATIONS.....	33
C.1.	Minimum Resolution Calculation.....	33
C.2.	Estimated PCB Data Size and Time Requirement	33
APPENDIX D:	IMAGE COLOUR CONTRAST SCALES	36
D.1.	Grey Colour Scale.....	36
D.2.	Dynamic Colour Scale 1.....	36
D.3.	Dynamic Colour Scale 2.....	36

Figures

Figure 2-1	X-Ray exposure set for focus on PCB under PGA. Red Circle: Tracks not under PGA are overexposed. Sample 3: Colour Bar Appendix D.3. 5
Figure 2-2	X-Ray exposure set for area around PGA. Red Circle: Exposure setting has centralised the tracks in the contrast. Sample 3: Colour Bar Appendix D.3. 5
Figure 2-3	X-Ray resolution set at 9 μm improves definition of internal tracks, Sample 3: Colour Bar Appendix D.3. 6
Figure 2-4	Hybrid RF encapsulated in steel housing. Red Circle: Thin film resistors harder to identify as Carbon is lower in the periodic table than Aluminium Oxide. Sample 2: Colour Bar Appendix D.2. 6
Figure 2-5	Hybrid RF encapsulated in steel housing with reduced maximum dynamic range of colours to between 7000 and 21000. Red Circle: Limiting the range is not able to bring more definition to the thin film resistors. Sample 2: Colour Bar Appendix D.2. 7
Figure 2-6	Transaxial cross-section image with 35 μm resolution and 5 degree rotation steps, Sample 3: Colour Bar Appendix D.3. 8
Figure 2-7	Transaxial cross-section image with 9 μm resolution and 0.5 degree rotation steps, Sample 3: Colour Bar Appendix D.3. 8
Figure 2-8	Nine micron slice of exterior and internal track layers with Sagittal and Transaxial views aligned to the bottom layer. Red Circle: variance in the track appearance through the slice. Green Circle: dense component producing noise through PCB layers. Sample 4: Colour Bar Appendix D.3. 10
Figure 2-9	Inductor coil inside steel case and encapsulated by potting compound. Inset top right in red: Scan area of Sample 1. Green Circle: Metal artifacts associated with denser materials containing lead. Colour Bar Appendix D.1. 11
Figure 2-10	Via and track connections of an internal layer. Red Circle: Noise present on track changes which material it is perceived as, making tight filtering harder. Sample 3. 12
Figure 2-11	Highlight of solder joints on small-outline integrated circuits (SOIC) to the PCB's pads. The metal frame inside the package interferes with observation under the package. Sample 3. 13
Figure 2-12	Observation of sample perpendicular to ground plane. Track features and vias can be resolved clearly but ground plane can barely be resolved. Red Circle: ground plane can be resolved by the lack of background noise. Sample 3. 14

DSTO-TR-2973

Figure 2-13	Observation of sample along the ground plane axis. Tracks features and connections to vias can be made out, however the ground plane has disappeared. Sample 3.	14
Figure 2-14	Anaglyph image (red/blue) representation allows easier interpretation of depth perception and internal layers, Sample 3.	15
Figure A-1	Illustration of streaking artifact production with a simulated water phantom. Top: parallel projection, filtered projection, and reconstructed images without error; bottom: about 10% error was added to three channels in a single projection at 45 deg [1].	19
Figure A-2	Illustration of the shading artifact production with the same water phantom as shown in Figure A-15. About 10% error was added to 40 channels in a single projection at 45 deg. (a) Profile of the erroneous projection. (b) Profile after filtering operation. (c) Reconstructed image [1].	20
Figure A-3	Illustration of the production of a ring artifact. About 1% of error was added to a single channel over all projection angles. (a) Projection profile with 1% added error. (b) Profile after filtering operation. (c) Reconstructed image [1].	20
Figure A-4	Illustration of a cause of partial volume artifact [1].	21
Figure A-5	Partial volume effect caused by the nonlinear logarithm operation (a) Thin slice and (b) non-thin-slice scanning [1].	22
Figure A-6	Example of the x-ray energy spectrum of an x-ray tube operating at 120kVp [1].	23
Figure A-7	X-ray mass energy spectrum for typical elements inside PCBs and hybrid packaged devices [8].	24
Figure A-8	Change of acceleration voltage leads to change of X-Ray energy, anode effectiveness, dose and spectrum [9].	25
Figure A-9	Change of current leads to change of X-Ray intensity (with no spectrum change) [9]	26
Figure B-1	Screen capture of the SkyScan 1076 interface page. On the left hand side of the image is the scout scan image. Central to the image shows a manual scan capture. Power settings can be seen underneath the radiation symbol.	29
Figure B-2	Reconstruction Algorithm Comparison [4]	32
Figure D-1	Grey Colour Scale	36
Figure D-2	Colour Bar Style 1	36
Figure D-3	Colour Bar Style 2	36

Tables

Table 2-1 Comparison of size and time of higher resolution quality
 reconstruction dataset with and without a ROI.....9

Table B-1 Configuration and result of the data collection on the SkyScan
 107631

ABBREVIATIONS / ACRONYMS

2D	Two Dimensional
3D	Three Dimensional
Al	Aluminium
Al ₂ O ₃	Aluminium Oxide
BGA	Ball Grid Array
Coronal	XZ Plane
COTS	Commercial Off The Shelf
C	Carbon
CT	Computed Tomography
DC	Direct Current
DSP	Digital Signal Processor
GPS	Global Positioning System
GPU	Graphics Processing Unit
IC	Integrated Circuit
MIP	Maximum Intensity Projection
PCB	Printed Circuit Board
PGA	Pin Grid Array
Pixel	Picture Element
QA	Quality Assurance
RF	Radio Frequency
ROI	Region Of Interest
Sagittal	XY Plane
SOIC	Small Outline Integrated Circuits
Ti	Titanium
TIFF	Tagged Image File Format
Transaxial	YZ Plane
VOI	Volume Of Interest
Voxel	Volumetric Pixel

1. Introduction

Over recent years the complexity of Printed Circuit Board (PCB) manufacturing has dramatically increased. Complex multilayer PCBs now dominate most of the latest electronic devices in use today. The multilayered architecture has allowed the top and bottom surfaces of the PCB to be used primarily for component mounting with the connecting tracks on the internal layers. The miniaturisation of electronic devices such as iPads and mobile phones has seen board layouts dramatically increase in density with distances between electrical contacts significantly decreasing. The complexity of the PCB depends on the fabrication process with some manufacturers producing boards with up to 35 layers containing tracks 25 μm wide separated by 50 μm . Buried vias, internal capacitors and resistors, newer type components such as BGA and flip-chip devices and flexible boards as thin as 75 μm are becoming more common. These complex multilayer PCBs present a challenge for testing and fault analysis with traditional methods becoming obsolete.

With the increase in PCB complexity the possibility of defects and faults has also increased. Defects and faults arise from both manufacturing and prolonged operation in the field. Some defects include: board delamination, broken conductors, dry solder joints, component misalignment and surface contamination by metal and ionic residues. Some manufacturing defects may escape detection by standard Quality Assurance (QA) testing and only appear during circuit operation in the field. PCBs operating under extreme environmental conditions such as high temperatures, humidity and atmospheric pressures, are vulnerable to developing defects over time. The need to not only identify the defect but to understand why it has occurred is crucial in designing fail-safe systems that can withstand harsh environmental conditions.

Two Dimensional (2D) X-ray imaging can assist in the identification of defects but is often time consuming due to the number of internal conductors on the PCB that may need to be examined. X-ray Computerised Tomography (X-ray CT) is primarily used in medical imaging but has recently been shown to be effective as a fault analysis tool in the PCB and semiconductor industry. The X-ray source rotates around the object producing a dataset of 2D X-ray slices. This dataset can be reconstructed into a full three dimensional (3D) image of the object including any internal layers of a PCB.

However, PCBs present their own challenge to CT systems due to the amount of dense material such as metal component frames, leads and solder in close proximity to very fine tracks. The absorption of X-ray radiation increases with atomic number and density. Therefore, areas of the PCB containing fewer dense materials may be overexposed while other areas with closely packed metal components and solder joints may be underexposed. A number of common artifacts that arise in the CT of PCBs include scatter, beam hardening, partial volume, streaking, shading, rings, bands and metal artifacts [Appendix A.1]. These artifacts can be reduced by optimising the scanning parameters to the sample or post processing.

CT systems also have been designed to remove artifacts by reducing the range of the materials analysed. Medical imaging CT systems, which make up the majority of the market, are focused on bone and soft tissue whilst achieving low doses of radiation.

Available material analysis CT systems are often more suited to imaging objects containing fewer metallic parts. The systems that can cope with objects containing many fine metallic structures in close proximity to larger denser materials are few and expensive. The *Phoenix L 300*¹ [5] for example has been designed for the PCB and semiconductor industry. It boasts a volumetric pixel (voxel) resolution of 0.4 μm and supports dual X-ray tubes which allows for high resolution imagery as well as 3D profiling of complete systems. There are many benefits that a high end system such as the *Phoenix L 300* can offer in the inspection and fault analysis of PCBs. However, there are also a number of disadvantages including initial expense, ease of use and on-going maintenance. Newer CT systems specifically designed for high density PCB analysis are becoming available and each system has its own unique features. Without a firm understanding of all the issues involved in CT of complex PCBs it is difficult to assess which type of system is best suited to the task.

2. Experiment

2.1 Experiment Objectives

Access to an offsite X-ray CT SkyScan 1076 system at Adelaide Microscopy provided the opportunity to analyse a number of sample PCBs. This allowed the issues involved to be investigated and allowed us to determine whether this technique could be used to identify and characterise certain defects on PCBs. The samples used in the experiments were multilayer PCBs. The experiment's objectives were to:

1. Determine if CT can be used on multilayered PCBs to identify certain defects and faults;
2. Investigate what effects the X-ray voltage and current, exposure time, frame averaging, filters, rotation step size and resolution have on the sample set and how to optimise these for particular PCBs;
3. Investigate the use of SkyScan software reconstruction tools to aid in the analysis of sample sets and which settings will optimise the results for the analyst;
4. With consideration of the experimental outcomes determine what features and specifications a suitable system should have for operational use.

2.2 Equipment Used

2.2.1 SkyScan 1076 micro-CT

The SkyScan 1076 is a high resolution low dose X-ray scanner for 3D reconstruction. The primary application for the SkyScan 1076 is to non-destructively scan small laboratory animals with detectable details down to 9 μm . The focus of the CT system is on biomedical analysis of soft tissue and bone. The SkyScan 1076 implements a circular step and shoot rotation pattern. The X-ray source rotates around the object producing a data set of 2D X-ray slices. This data set can be reconstructed into a full 3D image of the object including any internal layers of a PCB. The SkyScan 1076 is limited to a maximum sample size of 65 mm in diameter by 400 mm in length. The software only allows for 200 mm length scans at a time, so multiple scans may be needed for large samples [Appendix B.1]. For reconstruction requirements, the 2 mm

¹ Product information can be found as *Phoenix v | tome | x L 300*

bordering the images are removed from each scan when processing to create a full dataset and interleave stitching.

Aluminium (Al) and Titanium (Ti) filtering is available [Appendix B.1], which is required when scanning metal objects to remove Bremsstrahlung X-rays [1]. The scanning process is automatic and a batch processing feature enables repeated scans at the same settings at different locations, producing multiple datasets that are collected automatically. The SkyScan 1076 has three selectable resolution settings; 9 μm , 18 μm and 35 μm .

2.2.2 Nrecon Reconstruction Software

The Nrecon Reconstruction software converts a 16-bit Tagged Image File Format (TIFF) dataset (standard SkyScan output files) to a variable file format set of Transaxial (YZ plane) cross-section dataset. Some of the processing options available in the software allow the user to select: region of interest (ROI), beam-hardening, ring artifact reduction, smoothing and limit maximum and minimum contrast settings. The size of the cross-section of the image is dependent on the resolution size of the scanned data set (a 9 μm resolution size will have a cross-section slice of 9 μm). Nrecon can also use the additional 2 mm length of the scanned image to produce a larger dataset with partially reconstructed data.

The Nrecon Reconstruction software used is based on a modified Feldkamp algorithm for processing. The complexity of a typical Feldkamp algorithm is such that the computational time grows proportionally to the size of the dataset to the power of four [6]. Other processing algorithms exist that significantly reduce the processing time and are discussed in Section 2.4.2.

2.2.3 Analysis Software

SkyScan provides several analytical programs for use with their CT Scanners; of which DSTO was able to get free access to the DataViewer, CTvox and CTAn software. These programs respectively assist in; the reconstruction and examination of the 2D data, construction and inspection of 3D datasets and 2D/3D morphological operations and analysis.

The DataViewer software allows for viewing the data files created by both the raw output files and the Nrecon cross-sectional data set. It is also capable of creating cross-sectional data sets for the Sagittal (XY plane) and Coronal (XZ plane) planes sets out of the Transaxial data. The reconstructed dataset can be rotated in all dimensions and saved as a reduced subset of data for use with CTvox.

DataViewer is useful for observing flat surfaces and observing internal and exterior track layers when board warp is not present.

CTvox is a volume rendering program that converts the Nrecon pixel dataset into a voxel dataset which contains an emission colour and an opacity for each voxel. CTvox has three analysis functions; Volume rendering, Attenuation and Maximum Intensity Projection (MIP), which is discussed in Section 2.6.

CTAn is an analysis tool that calculates 2D and 3D morphometric parameters based on ROI and Volume Of Interest (VOI) of datasets. Adelaide Microscopy has a licensed version of CTAn, however the free version that was available had a limited feature set and therefore was not used.

2.2.4 PCB Samples

The range of samples used in the experiment represented the complexity of the PCBs that have developed faults in the field and required some form of post-trial analysis and testing. The samples were also chosen based on the maximum object size of the SkyScan 1076. Four PCBs were selected for the experiment:

Sample 1: DC-DC Converter with potting material enclosed in a steel housing

Sample 2: RF Hybrid with thin film resistors enclosed in a steel housing

Sample 3: Four layered DSP Processor Board with large components

Sample 4: Five layered PCB GPS Unit with ground planes top and bottom

2.3 SkyScan 1076 Configuration

The setup procedure for the experiment is described in Appendix B.3. For all datasets collected a filter was used to reduce the metal streaking artifacts. Most samples were scanned at maximum voltage and current, and by using the exposure time to change the contrast. By using the maximum current we were able to minimise the exposure time of the detectors, resulting in significantly faster runs. Using the highest acceleration voltage produces the highest peak energy spectrum output (Figure A-8), which helps avoid the non-linear attenuation region of the PCB materials (Figure A-7). The lowest resolution and frame averaging possible was used together with coarse rotation steps to reduce the dataset size and scan time. Frame averaging minimised background noise and scatter.

2.3.1 Contrast

The level of image contrast for each sample was optimised before scanning by varying the exposure time with the X-ray source at maximum power. This was checked both orthogonal to the top of the sample and rotated 60 degrees to observe that the sample's features were in the range of the detector's bandwidth. During setup, when the X-ray settings had been incorrectly set for a sample, over penetration would cause the detectors to be saturated whilst under penetration would cause photon starvation.

For Sample 3, the contrast bandwidth of the camera was not wide enough to observe through all the material densities. This was due to the acceleration voltage being limited to 100 kV on the SkyScan [Appendix B.1], and as a result the X-Ray was not able to further penetrate the sample, providing more image contrast. Since the Pin Grid Array (PGA) was still soldered to the PCB, the scanning parameters needed to be varied between observing under the PGA alone and the PCB around the PGA.

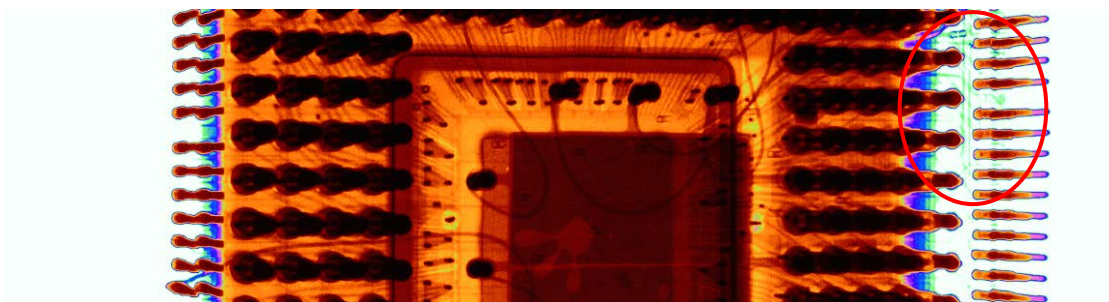


Figure 2-1 X-Ray exposure set for focus on PCB under PGA. Red Circle: Tracks not under PGA are overexposed. Sample 3: Colour Bar Appendix D.3.

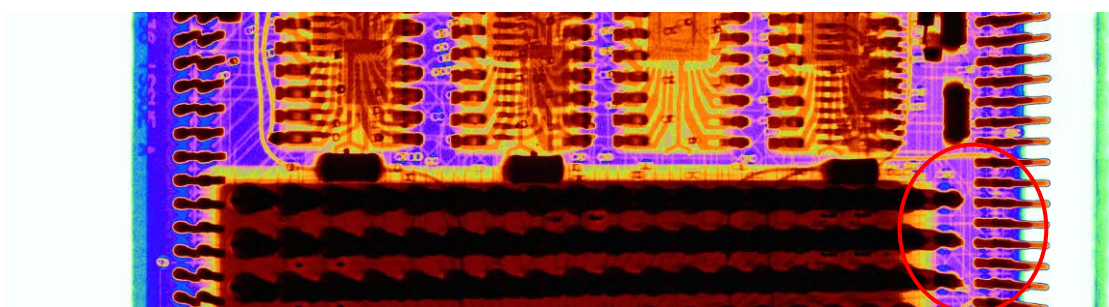


Figure 2-2 X-Ray exposure set for area around PGA. Red Circle: Exposure setting has centralised the tracks in the contrast. Sample 3: Colour Bar Appendix D.3.

Figure 2-1 and Figure 2-2 show the variation in the contrast of the PCB image, in particular the tracks. The exterior track width is sufficiently wide enough for observation under good contrast (Figure 2-2), however it can be degraded by poor contrast (Figure 2-1). Having an excessive acceleration voltage causes over penetration through the less dense sample material to contribute to the surrounding dense material's photon count. This causes an image misinterpretation of the edges of the dense material, which results in the operator causing a partial volume effect (Appendix A.1.2).

Some tracks will become better resolved as the angular position changes throughout the scan when the change in attenuation in the surrounding material increases the track intensity. The exposure times recommended for PCBs are dependent on the amount and type of components on the board. From the experiment results, a densely populated PCB such as that shown in Figure 2-1 needed around 700 ms of exposure time while an unpopulated/sparse board required only 300 ms with a 35 μm resolution. In general, the amount of exposure time needed is inversely proportional to the resolution of the scan. Therefore, as the complexity of the PCB is reduced so is the required exposure time.

2.3.2 Resolution

At lower resolution settings, neighbouring array cells in the detector are clustered together to increase the effective size of a cell. This reduces the required exposure time [1]. Increasing the detector resolution splits the array into individual cells resulting in darker images due to a decrease in the photons per unit area. This

requires a longer exposure to the X-ray source to produce a suitably contrasted image.

In Figure 2-3 the increase in sampling from the improved spatial resolution has made the internal tracks in the reconstruction more rigid. This is because the dataset contains more detail resulting in the reconstruction algorithm and analysis stages not filtering out the tracks as noise.

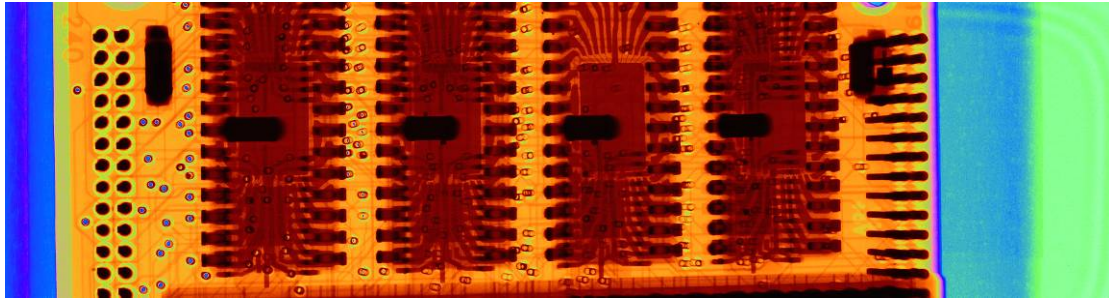


Figure 2-3 X-Ray resolution set at 9 μm improves definition of internal tracks, Sample 3: Colour Bar Appendix D.3.

The internal tracks of Sample 3 at 100 μm wide demanded the smallest resolvable detail compared to any other structures on the PCB. At 9 μm resolution there are 11 pixels of data to resolve the track, but for the standard 35 μm resolution scan there are only 2 pixels. Both pixels may be subjected to the partial volume effect, which causes blurring around sharp edges that may result in the track not being resolved. At least another 3 pixels not subjected to partial volume effect would be needed for the post-processing to resolve the tracks sufficiently to determine any significant damage such as a break.

2.3.3 Dynamic Colour Range

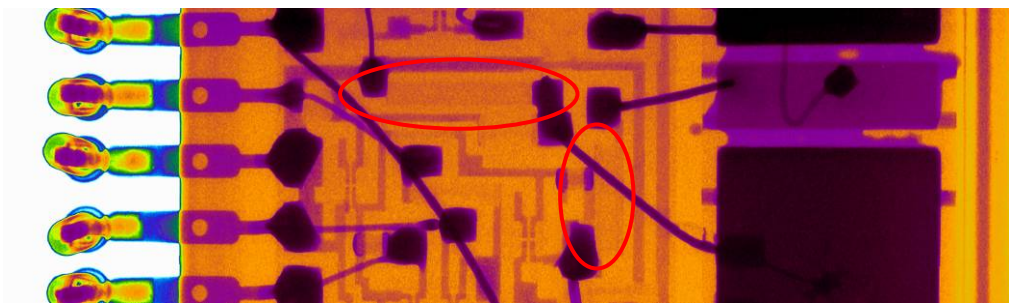


Figure 2-4 Hybrid RF encapsulated in steel housing. Red Circle: Thin film resistors harder to identify as Carbon is lower in the periodic table than Aluminium Oxide. Sample 2: Colour Bar Appendix D.2.

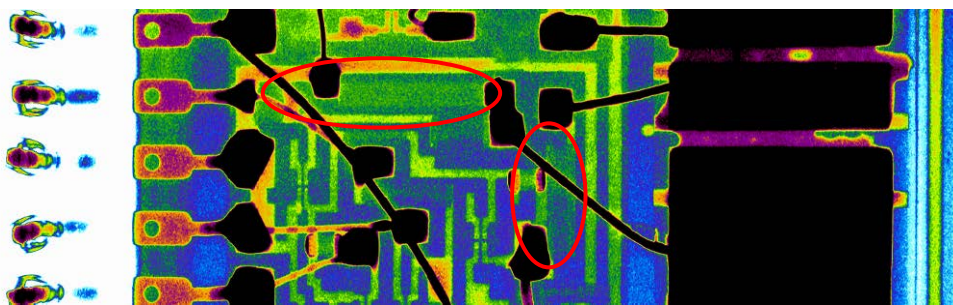


Figure 2-5 Hybrid RF encapsulated in steel housing with reduced maximum dynamic range of colours to between 7000 and 21000. Red Circle: Limiting the range is not able to bring more definition to the thin film resistors. Sample 2: Colour Bar Appendix D.2.

When multiple materials need to be analysed, the SkyScan range can differentiate between elements whose atomic mass varies by more than 1% [4]. Determining shape becomes difficult as seen in Figure 2-4 and Figure 2-5, where the Carbon (C) thin film resistor on the Aluminium Oxide (Al_2O_3) substrate is only just visible at a particular angle. The small viewing range of these thin film resistors makes it difficult to reconstruct them in the cross-sectional data, as post processing is likely to filter them out as noise. Although time did not permit, further scans at higher resolution and contrast settings optimised for carbon (Figure A-7) are likely to better reveal these thin film resistors.

2.3.4 Metal Artifacts

Streak artifacts created by metal structures become significant and can have a large influence on the construction of the cross-section dataset. The most significant of these artifacts are dark streaks between high density materials which are surrounded by bright streaks, which appear similar to tracks. Variations in the appearance of certain artifacts are dependent on other contributing artifacts. The causes, appearances and reduction techniques of these artifacts are summarised in Appendix A.1.

Beam hardening artifacts were a major component of the artifacts present during scanning; due to the large volumes of separate metal tracks in the PCBs. These artifacts can be reduced using two methods. In the first method the electron acceleration voltage is increased, which in turn increases the maximum X-ray spectrum produced (Figure A-8). The second method involves adding filtration between the X-ray source and the sample to remove the lower energy part of the X-ray spectrum. Together these reduction methods move the material absorption away from the exponential region to the linear absorption region (Figure A-7) in the X-ray spectrum [1:Chapter 7].

For this reason most samples were scanned at the maximum available electron acceleration voltage and current. Varying the exposure time in an attempt to reduce metal artifacts can be successful but care is needed not to introduce operator artifacts such as improper contrast. The X-ray source filtration selected was the Al 1 mm plate which not only reduced the background metal artifacts such as Poisson noise and scatter greater than the Al 0.5 mm plate, but also reduced the X-ray output.

Reduction of the exposure time was also considered important as this reduced the overall scan time.

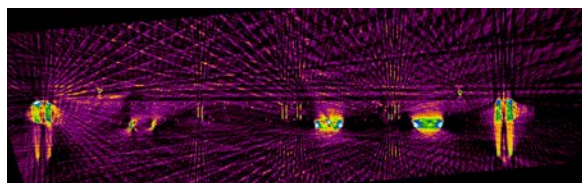


Figure 2-6 Transaxial cross-section image with 35 μm resolution and 5 degree rotation steps, Sample 3: Colour Bar Appendix D.3.

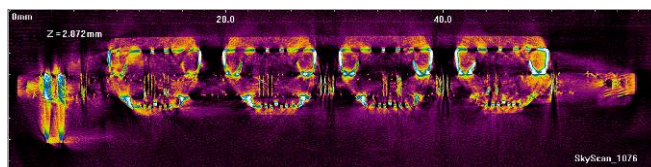


Figure 2-7 Transaxial cross-section image with 9 μm resolution and 0.5 degree rotation steps, Sample 3: Colour Bar Appendix D.3.

In Figure 2-6 there is considerable windmill streaking occurring from the metal inline header pins and solder on the board. The fanning out of the streaking is representative of the rotation step size taken. For Figure 2-7 it can be seen that the streaking distance has been reduced considerably by increasing both the image resolution and increasing the number of samples collected. The reduction in scan time by reducing the rotation steps appeared to be the best trade off considering the quality of data and dataset size reduction. However, for a high quality dataset a rotation step size below 0.7 degrees per step is recommended.

2.4 Cross-section Reconstruction Configuration

2.4.1 Software Artifact Reduction

By calibrating the Nrecon Reconstruction software to the individual dataset it is possible to reduce or remove some consistent artifacts generated by the SkyScan 1076. The effects that can be reduced include beam-hardening, noise and ring artifacts. However these software tools are mainly optimised for medical imaging. Exploration of the reduction techniques was both computationally and time expensive with the software available and required fine adjustment to parameters for poor quality datasets.

2.4.2 Computational Power

To ensure only the area of interest in the dataset is processed, a ROI can be selected in the X, Y and Z planes. This will significantly reduce the amount of disk space needed for processing since PCBs are typically flat in one dimension. A smaller reconstructed dataset allows the CTvox and DataViewer tools to load and navigate the sample dataset quicker. Under sampling is another option to reduce the size of the dataset, however this also reduces the resolution which in turn may detrimentally affect the visibility of smaller internal tracks (Section 2.3.2). Datasets

can also be segmented into smaller ROI so the analysis tools are able to cope with larger data sizes.

Table 2-1 Comparison of size and time of higher resolution quality reconstruction dataset with and without a ROI

Dataset	Raw Dataset	ROI Reconstruction	Without ROI Reconstruction
Sample 4	4.62GB	28GB (84min)	384GB
Sample 3 - Internal layer	22.1GB	19.3GB (17hrs)	

Table 2-1 shows the amount of physical disk space required for the data from each sample. Without the selection of a ROI a large amount of physical memory will be needed to store the cross-sectional dataset.

The SkyScan's Nrecon Reconstruction is also available in several different versions that permits computer clustering, use of a Graphics Processing Unit (GPU) accelerated algorithm and an optimised smaller set algorithm. These options will reduce the time taken to process by between 4 to 50 times depending on the computer hardware and algorithms (Appendix B.5).

2.5 2D Cross-section Results

The 2D cross-sectional results from the reconstructed dataset can be loaded into DataViewer which will then interpolate the Coronal and Sagittal axes from the Transaxial reconstructed dataset. The DataViewer program can be aided by the use of GPU accelerators, which speed up the viewing process. However, image processing actions such as rotation and alignment of the dataset will require large amounts of memory and processing.

2.5.1 Board Warp and Flatness

In Figure 2-8 below, it can be seen that the tracks are more observable on the exterior layers and that the tracks are not continuous in attenuation. Some of the attenuation can be seen in other Sagittal slices which are 9 μm apart. As the resolution of the scan increases similarly the number of slices that are taken to observe layers is increased. The variations in the track attenuation can be attributed to board warp, misalignment of the sample positioning and surface components changing the attenuation. During the analysis process, variations make it difficult to follow a discontinuous track without navigating adjacent slices. Denser components can also be seen projecting through slices in the PCB.

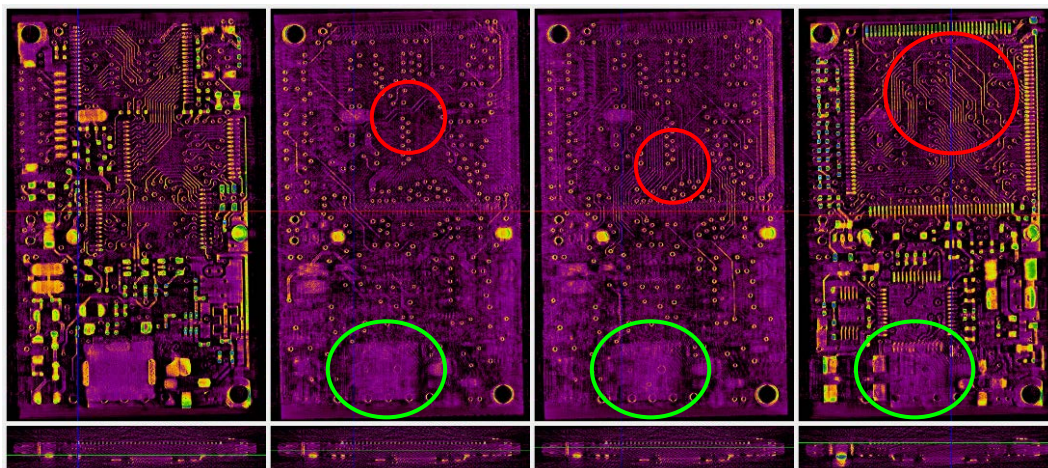


Figure 2-8 Nine micron slice of exterior and internal track layers with Sagittal and Transaxial views aligned to the bottom layer. Red Circle: variance in the track appearance through the slice. Green Circle: dense component producing noise through PCB layers. Sample 4: Colour Bar Appendix D.3.

Identifying board warp will be easier to observe under slice operations but non flat PCB layers cannot be observed in a single slice. This can be improved by collating track data from multiple slices for PCBs with minimal board warp. The Coronal and Sagittal images produced by the DataViewer can be saved as individual datasets upon reconstruction, which further reduces the dataset for 3D reconstruction.

2.5.2 Continuity

From Figure 2-9, it can be seen that the wound inductor coil wire does not interfere with itself (no beam-hardening artifact) so the continuity of the line can be observed. The ability to rotate around the central axis of the inductor allowed for quick observation of the wire. Metal artifacts are more predominate in the sample around the denser metal objects such as the solder and the resistor leg.

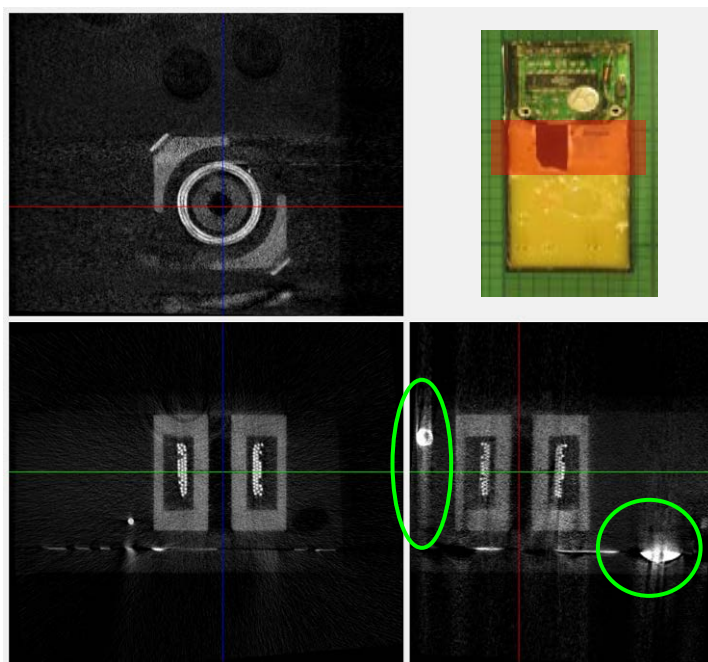


Figure 2-9 Inductor coil inside steel case and encapsulated by potting compound. Inset top right in red: Scan area of Sample 1. Green Circle: Metal artifacts associated with denser materials containing lead. Colour Bar Appendix D.1.

2.6 3D Reconstruction Model Results

The 2D cross section results from the reconstructed dataset can be loaded into the CTVox software which creates a 3D volume model that selects a blending mode. The blending modes available with CTVox are Volume, Attenuation and Maximum Intensity Projection (MIP). Inside the 3D volume model, each voxel in the dataset contains information on the opacity and emission. CTVox allows for the appearance of all equivalent voxels to be changed by the use of transfer functions. Using the transfer function to control the opacity values allows the analyst to set the transparency of each voxel. Similarly control of the emission transfer functions allows the colour of each voxel to be changed.

For 3D reconstruction, the software package requires enough onboard GPU memory to open the size of the cross sectional dataset as a minimum requirement to open the dataset. As a consequence the larger datasets were not able to be completely opened since the GPU memory was not large enough.

2.6.1 Volume Rendering

Volume rendering is good for interrogating surfaces with the use of the slice tool, optical transfer functions and lighting. Setting up the transfer functions for emission and opacity requires time to be spent focusing on correctly attenuating unwanted materials and colouring desired projection. The navigational tools allow for the orientation and position of the object, and the rotation and selection of the camera viewing angle.

The slice tool is used for cutting and clipping shapes out of the object to observe underlying materials. Inside the CTVox program there is one object clipping box that displays the 3D dataset object inside and another selectable shape that can be used for cutting or clipping. This tool allows for the individual observation of loaded components, individual layers and cross sections with depth. The use of this tool is needed for complex, multilayered and dense PCB designs, as it enables focusing on a Volume Of Interest (VOI).

The transfer functions for opacity changes the transparency of materials whilst the emission colour displayed changes depending on how much the material absorbs the X-ray radiation. This requires lots of fine tuning for observation of internal tracks, vias and exterior tracks simultaneously, as it involves tuning out the PCB substrate whilst keeping as much of the metal structures as possible. This becomes harder with poorer quality datasets as the noisy metal tracks get filtered out as substrate material or background noise. Changing the red, blue and green emission colouring can help with the identification of noisy features such as tracks as seen in Figure 2-10.

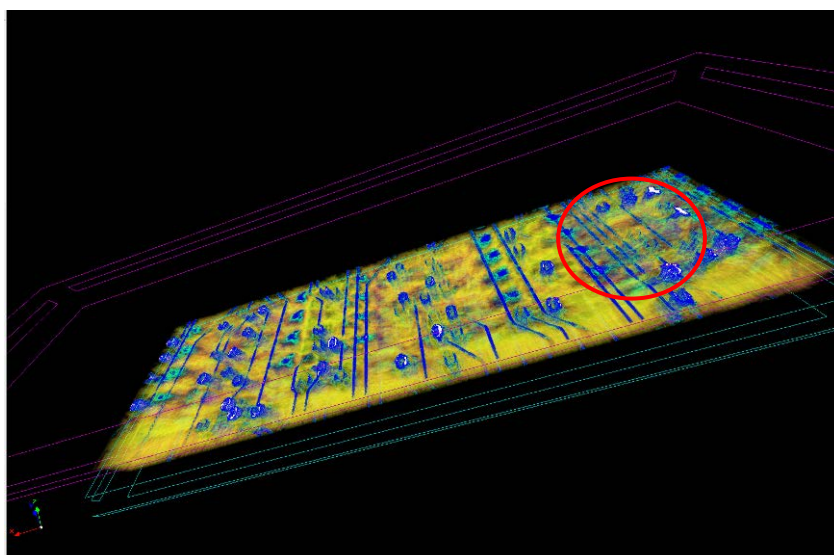


Figure 2-10 Via and track connections of an internal layer. Red Circle: Noise present on track changes which material it is perceived as, making tight filtering harder. Sample 3.

In Figure 2-10 the internal via connections to the tracks can be seen with the assistance of slice tools and the optical transfer functions. The transfer functions have been set to make the sample appear semi-solid whilst the emission profile was changed to display blue for heavily attenuating materials, green for lightly attenuated and the substrate as yellow. The colour scheme was particularly helpful for assessing the continuity of internal tracks when streaking had occurred. Volume rendering was found to be helpful for confirming solder connections as shown in Figure 2-11, but further work needs to be done to remove the metal internal to the Integrated Circuit (IC) for observation of the PCB.

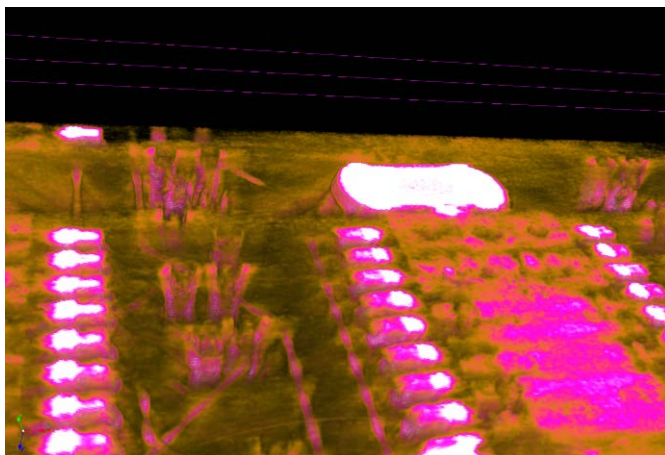


Figure 2-11 Highlight of solder joints on small-outline integrated circuits (SOIC) to the PCB's pads. The metal frame inside the package interferes with observation under the package. Sample 3.

2.6.2 Attenuation Rendering

Attenuation rendering produces a digitally reconstructed radiograph along the current viewing direction which is similar to the CT scanner raw image file. This may be useful for a 3D navigation of the sample to determine the best orientation for the sample inside the CT scanner. This blending mode is not particularly useful for observation of PCBs as it requires the depth of the material to provide the contrast intensity.

2.6.3 Maximum Intensity Projection

Maximum Intensity Projection (MIP) retains only the most intense voxel along each ray for every ray present on the screen. The MIP opacity and emission data visualisation highlights dense materials and metal objects significantly. This requires less adjustment of the configuration settings in order to observe fine structures such as small internal tracks. This helps in the reduction of post-processing and configuration as it removes the need to take out the substrate or other nearby heavily attenuating materials which can make observing the smaller tracks difficult.

Determining power and ground plane connections to vias using MIP is not ideal as only the most intense voxel is kept. Positioning the camera perpendicular to the ground plane in Figure 2-12 was the easiest way to determine the planes connection to the vias. The vias lack of connection to a plane can be shown by a dark ring around the via from the background noise.

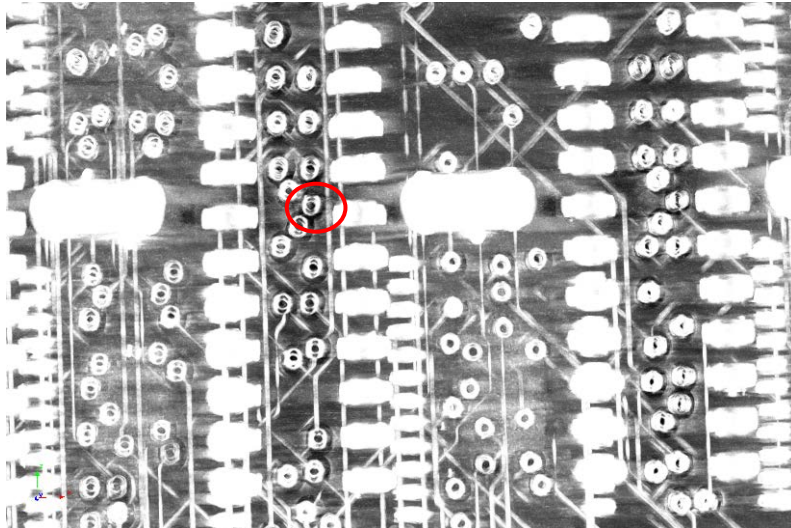


Figure 2-12 Observation of sample perpendicular to ground plane. Track features and vias can be resolved clearly but ground plane can barely be resolved. Red Circle: ground plane can be resolved by the lack of background noise. Sample 3.

Observation of the ground plane itself using the slice approach with MIP was not successful. This can be seen in Figure 2-13. Internal tracks and their connections to the vias are visible but the ground plane connections are not distinguishable.

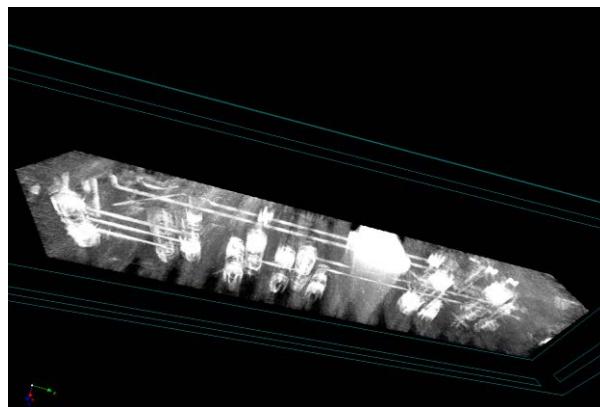


Figure 2-13 Observation of sample along the ground plane axis. Tracks features and connections to vias can be made out, however the ground plane has disappeared. Sample 3.

CTVox is also capable of producing stereo vision (anaglyph image) of the objects which provides depth perception with a pair of red/blue glasses. This observational tool works well with MIP as substrate materials have been removed. Using stereo vision allows for the observation of more complex objects present in a flat image as the depth perception provides more information about the location of features.

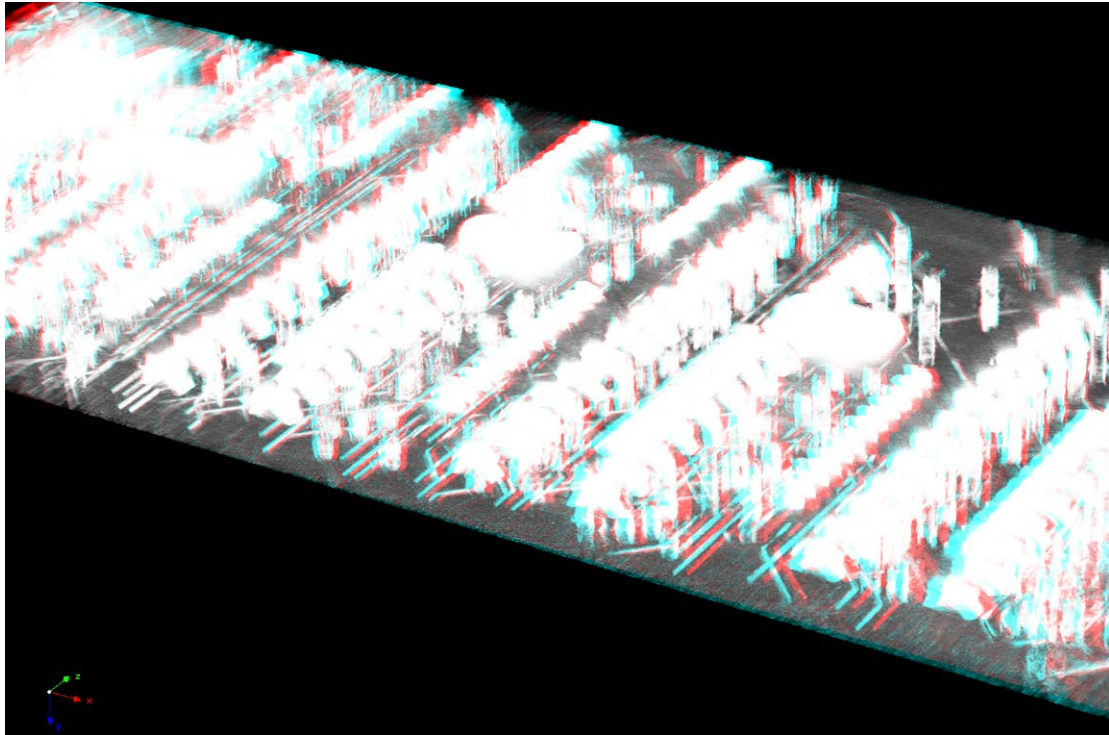


Figure 2-14 Anaglyph image (red/blue) representation allows easier interpretation of depth perception and internal layers, Sample 3.

3. Conclusions

This experiment has highlighted some of the issues involved in using a SkyScan 1076 X-ray CT system as a non-destructive technique to analyse multilayer PCBs. The experiment showed that CT can be used on multilayered PCBs to identify certain defects and faults provided the minimum analysis requirements are met by the CT system. It also showed the importance of using the appropriate software reconstruction tools to aid in the analysis of sample sets. A number of PCBs were used in this experiment that contained a variety of hard to scan features including small tracks within areas of dense metallic structures and solder joints. The range of samples used allowed a broad assessment of the issues involved in using CT to conduct fault analysis on complex multilayered boards. The experiment has highlighted the importance and the time taken to correctly process the data sets to obtain suitable reconstructed 3D images. It has also shown the advantages and disadvantages between CT and real-time X-ray imaging. A number of issues were identified which significantly affected the ability to produce workable 3D images including various artifacts common to both CT and real-time X-ray. The following guidelines outline how to effectively use CT as a non-destructive technique to analyse multilayer PCBs:

High Quality Datasets

Obtaining a high quality dataset of the sample minimises the amount of post processing needed but is initially very time consuming. Most of the common artifacts can be reduced at scan time to produce high quality datasets. The

reconstruction software will stand a better chance in resolving the smallest structures needed to be observed using a high quality dataset.

Define the analysis requirements

Depending on the required task an entire PCB may not need to be scanned or alternatively a lower resolution and larger step size may be used. If the general location of a defect or fault is known then scanning a smaller area at the appropriate resolution will yield a smaller dataset which will be quicker and easier to reconstruct. Furthermore, the smaller the scanned area the less the variation in material densities that can cause exposure problems and common artifacts. Use of the slice tools in the analysis programs will also minimise the clutter and be able to focus on faults.

The object size itself may determine what type of CT system needs to be used. Generally, in single source CT scanners, the higher the resolution the smaller the maximum object size. The SkyScan could accommodate a maximum object size of 400 mm x 68 mm. However, dual source systems are available that boast high resolution and the ability to scan large objects.

Setting the scan parameters to the sample

Optimising the scan to the sample significantly reduces the artifacts associated with densely populated PCBs. Some of these artifacts, such as windmill streaking can be almost eliminated, resulting in a high quality dataset. It may be necessary to scan the same location with different settings to account for boards with wide ranges of material densities. Multiple scans of the same areas would allow the PCB containing large amounts of dense materials and those areas containing few dense structures are able to be scanned at the optimal settings.

Source filtering

Source filtering should be used when metal is present in the sample, which is generally always for PCBs. Depending on the abundance of metal artifacts, various aluminium filters can be selected to filter the X-ray source. This reduces the lower X-ray spectrum produced. Other filters may exist that may keep only the higher energy sections of the X-ray spectrum.

Increase frame averaging

By increasing the frame averaging, noise produced by some common metal artifacts can be reduced. Some tracks may require more frame averaging as they enter dense, noisy regions of the board.

Increase the electron acceleration voltage

Higher X-ray energies will penetrate dense materials further than those of lower energies. Some metal artifacts resulting from under penetration can be reduced this way. Lower energy X-rays are prone to rapid absorption which can lead to misdiagnosis of the material.

Adjust the contrast of the image

Adjusting the current and exposure time (as well as voltage) can optimise the contrast to the density of the sample area being scanned.

Set an appropriate resolution

The resolution of the scan should be set for the desired finest resolvable feature in the scanning plane; for PCBs this is track width. Low resolution may result in some fine structure not being resolved such as internal tracks. However, reducing the resolution significantly reduces the size of the data set making reconstruction and post processing quicker. Using a 10 μm resolution would be sufficient for a 100 μm wide track.

Set an appropriate step size

Generally, the lower the resolution the larger the step size, resulting in a smaller sized dataset. However, in the experiment it was found that a step size of at least 0.7 degrees was required for acceptable datasets even with resolutions as large as 35 μm . As this resolution increases there will be more images to process which will increase spatial resolution, in particularly further away from the isometric-centre of the scan [1].

Adjust the exposure time

Denser areas on PCBs require longer exposure times compared to sparse areas. Over-exposure of an area containing few dense components can result in fine structure such as small internal tracks becoming obscured. The exposure time can be adjusted for single individual scans but must be set to specific values in a CT scan.

Utilise dedicated software processing tools

Most common artifacts can be reduced at scan time to produce high quality datasets. However, on complex PCBs there will always be some remaining artifacts and noisy areas. Processing tools that permit changing the emission colouring can help to identify weak objects. Most software reconstruction tools can be computationally expensive and large datasets are memory expensive. Initially obtaining high quality datasets significantly reduces the burden on post processing.

Reconstruction and post-processing software continues to advance with the number of available third party tools increasing. Some of these tools are specifically designed for complex materials analysis such as PCBs. This will undoubtedly result in both a better quality reconstructed image as well as a significant reduction in the time taken to produce the 3D projection.

CT as a non-destructive technique to analyse multilayer PCBs already has a number of big advantages over real-time X-ray. Although there are also a number of issues that have been identified in this experiment, most of these are likely to be resolved with the advancement of technology. Already processing times for reconstruction have been slashed with the advance in GPU cluster computer systems. Dual source

systems have enabled both high resolution and large maximum object sizes, advances in processing software have allowed material identification, and artifact and noise reduction in complex PCBs.

4. Acknowledgements

We would like to thank Ruth Williams, Adelaide Microscopy for her assistance with the Micro CT.

5. References

1. Jiang Hsieh: Computed Tomography, Second Edition: Principles, Design, Artifacts, and Recent Advances (Published by Society of Photo-Optical Instrumentation Engineers, 2009)
2. F.P. Gentile, F. Sabetta, V. Troi: Computerised Axial Tomography (CAT) (Published by Defence Research Information Centre Glasgow, 1990)
3. F Edward Boas, Dominik Fleischmann: CT artifacts: Causes and reduction techniques (Published Imaging Med. (2012) 4(2), 229-240)
4. SkyScan Range reconstruction time comparison - volumetric reconstruction www.skyscan.be/products/nrecon.htm
5. General Electric CT range - Phoenix v|tome|x L300 www.ge-mcs.com/en/radiography-x-ray/ct-computed-tomography.html
6. S. Xiao, Y Bresler, D.C. Munson: Fast Feldkamp Algorithm For Cone-Beam Computer Tomography (Released 2003 University of Illinois)
7. L.A. Feldkamp, L.C. Davis, J.W. Kress: Practical Cone-Beam Algorithm (Published by Journal of the Optical Society of America A (1984) Vol.1 Issue.6 612-619)
8. J.H. Hubbell, S.M. Seltzer: Tables of X-Ray Mass Attenuation Coefficients and Mass Energy-Absorption Coefficients from 1 keV to 20 MeV for Elements Z = 1 to 92 and 48 Additional Substances of Dosimetric Interest (Published by Radiation and Biomolecular Physics Division, PML, NIST, 1995)
9. S.Tabalov: X-ray Tube and Generator - Basic principles and construction <http://www.elecinfo.com/upload/community/2014/01/15/1389777522-96281.pdf>

Appendix A: X-Ray Physics

A.1. Artifact Summary

The following artifacts have summarised from the resources [1,3].

A.1.1 Appearances of Image Artifacts

Streaking

Appearance	- Bright or dark streaks across the reconstructed image
Cause	- Inconsistency with an isolated measurement - Aliasing streak is determined by insufficient resolution
Algorithm Problem	- Individual projection amplifies a singular overshoot to be in between two undershoots
Imaging Problem	- In large quantities will corrupt the dataset lowering the outcome resolution quality or making the dataset unreadable

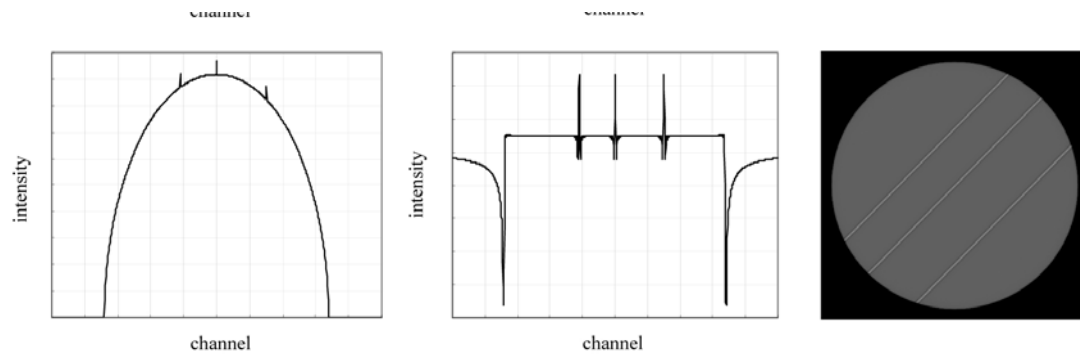


Figure A-1 Illustration of streaking artifact production with a simulated water phantom. Top: parallel projection, filtered projection, and reconstructed images without error; bottom: about 10% error was added to three channels in a single projection at 45 deg [1].

Shading

Appearance	- Smooth bright or dark continuous band across the image, can be localised to around the object or be a larger projection
Cause	- Tend to occur near objects of high contrast
Algorithm Problem	- Deviation of a group of detector measurements - Smoother overshoot and undershoot as there is less discontinuities with the surrounding channels
Imaging Problem	- Objects can appear shadowed near dense materials which may reduce the intensity and change the identification of the object

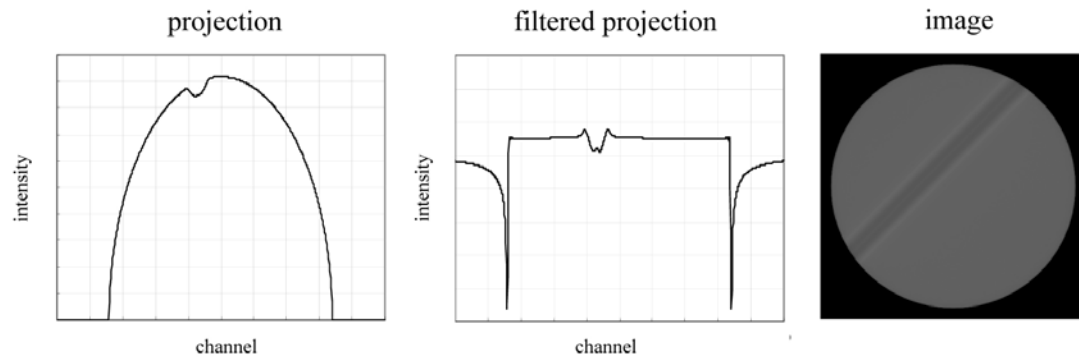


Figure A-2 Illustration of the shading artifact production with the same water phantom as shown in Figure A-15. About 10% error was added to 40 channels in a single projection at 45 deg. (a) Profile of the erroneous projection. (b) Profile after filtering operation. (c) Reconstructed image [1].

Rings and Bands

Appearance	- Appears as either full rings, arcs or as a central smudge across the reconstructed image
Cause	- Consistent incorrect detector readings over scan
Reduction method	- Acquisition of a flat field image with an aged X-ray source for calibration
Imaging Problem	- In large quantities the artifact will corrupt the dataset lowering the quality of the dataset or make it unreadable

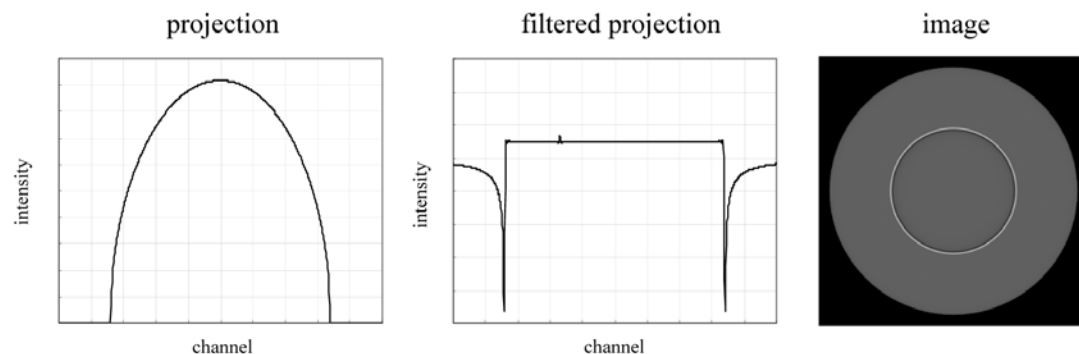


Figure A-3 Illustration of the production of a ring artifact. About 1% of error was added to a single channel over all projection angles. (a) Projection profile with 1% added error. (b) Profile after filtering operation. (c) Reconstructed image [1].

Other artifacts exist which can be special cases which do not fall into these categories.

A.1.2 System Design Artifacts

Aliasing

- | | |
|-------------------|---|
| Causes | - The maximum frequency contained by the CT signal is limited by the focal spot size, scanner geometry and the detector cell size |
| Reduction methods | <ul style="list-style-type: none"> - Sample the data at least twice the highest spatial frequency contained by the PCB (Shannon sampling criterion /Nyquist sampling criterion) - Different source and detector path lengths to produce extra samples (adds cause to partial volume effect) |

Partial volume effect

- | | |
|-------------------|---|
| Causes | - Projection inter-view inconsistency and intra-view inconsistency |
| Reduction methods | <ul style="list-style-type: none"> - Use thinner slices when high variations in object attenuation - Keep sample as close to the isometric centre of the CT scanner as possible (Introduced by extra sampling from aliasing) |
| Imaging Problem | <ul style="list-style-type: none"> - Edges of high density material losses definition (blurring) and blends with surrounding density material. Increases the resolution requirement for observing high density material in sparse low density material - Streaking near sharp objects - Rings and bands for sharp objects away from the isometric centre |

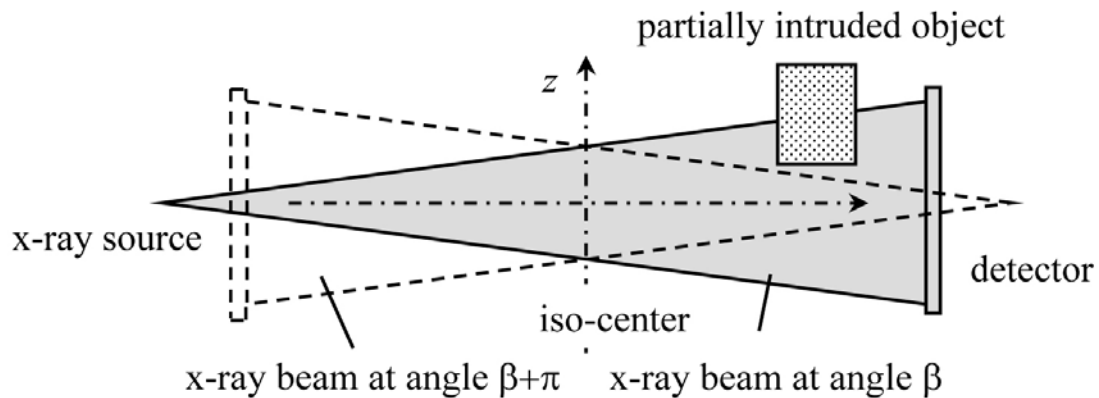


Figure A-4 Illustration of a cause of partial volume artifact [1]

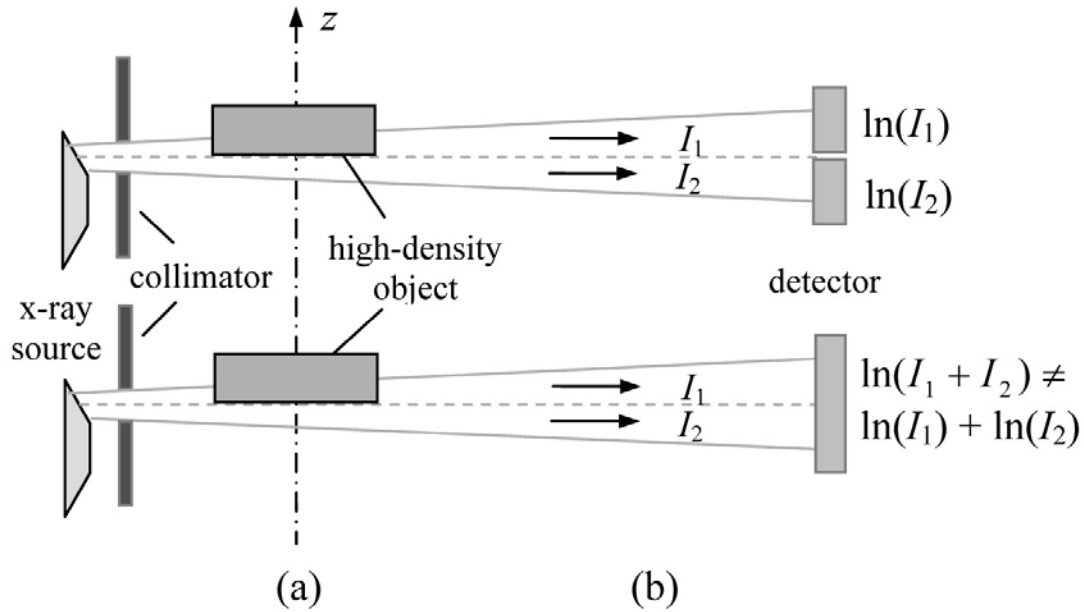


Figure A-5 Partial volume effect caused by the nonlinear logarithm operation (a) Thin slice and (b) non-thin-slice scanning [1].

Scatter

Causes

- Primary x-ray photons can scatter off objects and end up on other detectors (Compton scatter or incoherent scatter)

Reduction methods

- Frame averaging over multiple samples

Imaging Problem

- Algorithm reconstruction assumes that photon projections are linear
- Signal measured by detector represents the integrated X-ray flux over the sampling period
- Intensity shifts, shading or streaking artifacts

A.1.3 Sample Based Artifacts

Beam Hardening

Causes	<ul style="list-style-type: none"> - Polychromatic and broad x-ray beam spectrum and energy-dependent attenuation coefficients for samples - Detector attenuation is the sum of all spectra over absorption range (analysis of multiple dense materials becomes harder)
Reduction methods	<ul style="list-style-type: none"> - Apply filters of aluminium, copper or brass to attenuate low energy photons (spectrum conditioning) between source and object - Increase X-ray energy to shift energy-dependent attenuation into the linear region (move spectrum away from exponential attenuation curve for each materials) - Software corrections can be made (predominately based for water attenuation which is similar to soft tissue)
Appearance	<ul style="list-style-type: none"> - Dark banding between dense objects (Shading) - Fuzziness of light density objects near dense objects

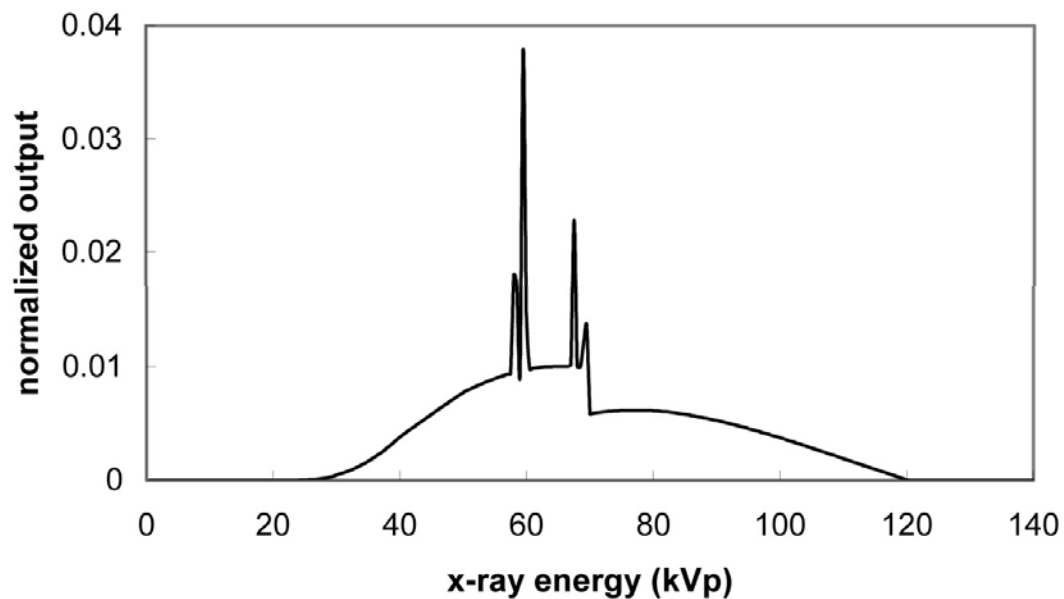


Figure A-6 Example of the x-ray energy spectrum of an x-ray tube operating at 120kVp [1]

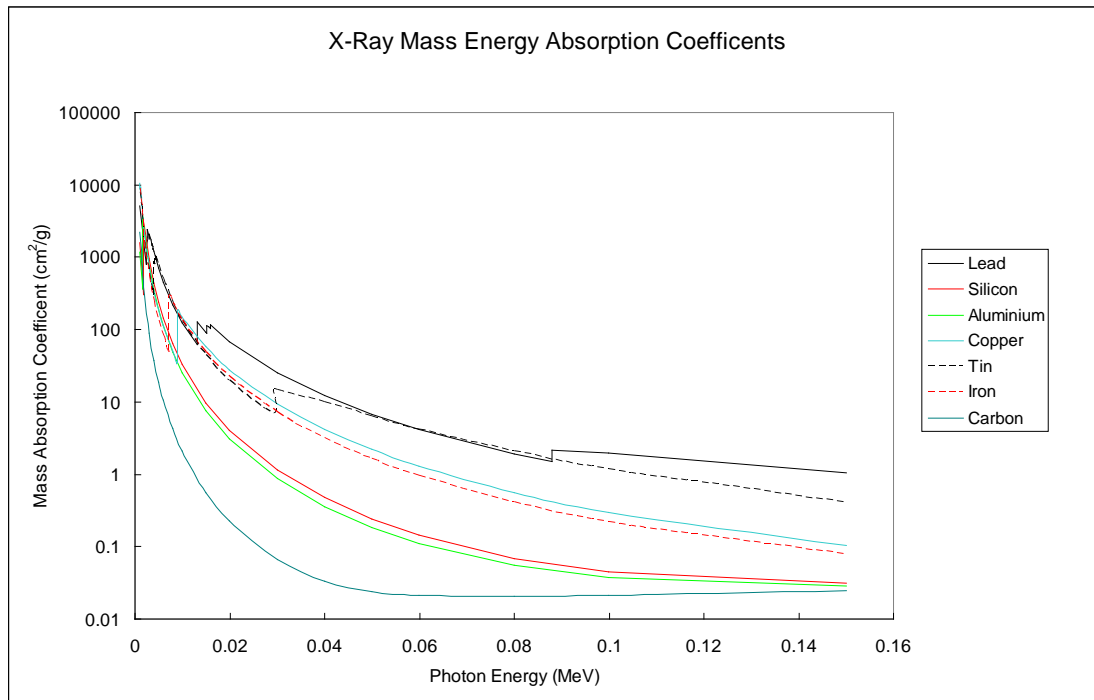


Figure A-7 X-ray mass energy spectrum for typical elements inside PCBs and hybrid packaged devices [8]

Metal Artifacts

Metal artifacts vary based on the metal itself and the metal edges

Causes

- The metal itself causes beam hardening, scatter effects and Poisson noise
- Metal edges cause streaks due to under sampling (aliasing), motion, cone beam (SkyScan 1076) and windmill artifacts

Reduction methods

- Previously discussed reduction methods

Imaging Problem

- Shading, streaking, blurring, rings and bands and fuzziness

A.2. Definitions

Pixel	(Picture Element) Point data source within a 2D array containing opacity information
Voxel	(Volumetric Pixel) Point data source within a 3D array containing opacity information

Generated X-Ray Sources:

Bremsstrahlung	Electron does not stop at the anode, and ejects a photon from the deceleration from the change in path (braking radiation)
Stopping Radiation	Electron transfers all energy to the transmitted photon that was produced between the cathode and the anode, stopping at the anode

A.2.1 X-Ray Spectrum

The X-ray spectrum produced from the electrons can be altered by changing both the acceleration and the amount of electrons. Spikes in a consistent X-rays spectrum are from the stopping radiation, which will not shift in energy unless the anode material is changed. The peak from Bremsstrahlung radiation changes dependant on the acceleration voltage will shift the peak of spectrum.

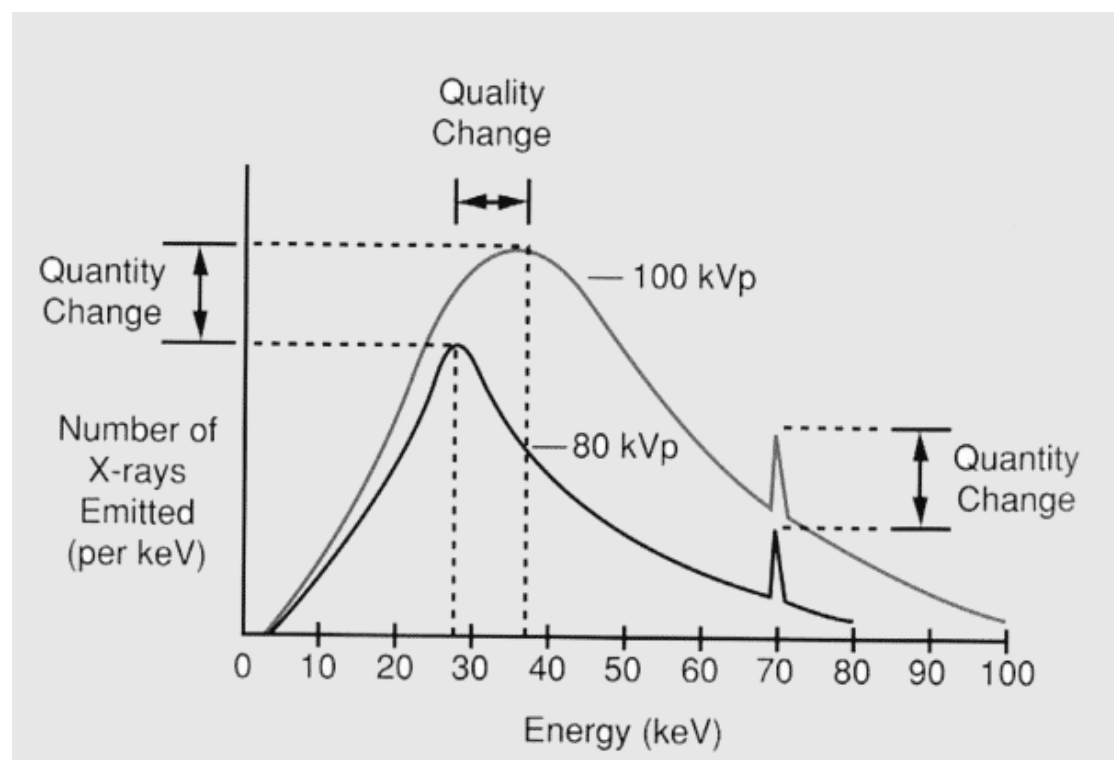


Figure A-8 Change of acceleration voltage leads to change of X-Ray energy, anode effectiveness, dose and spectrum [9]

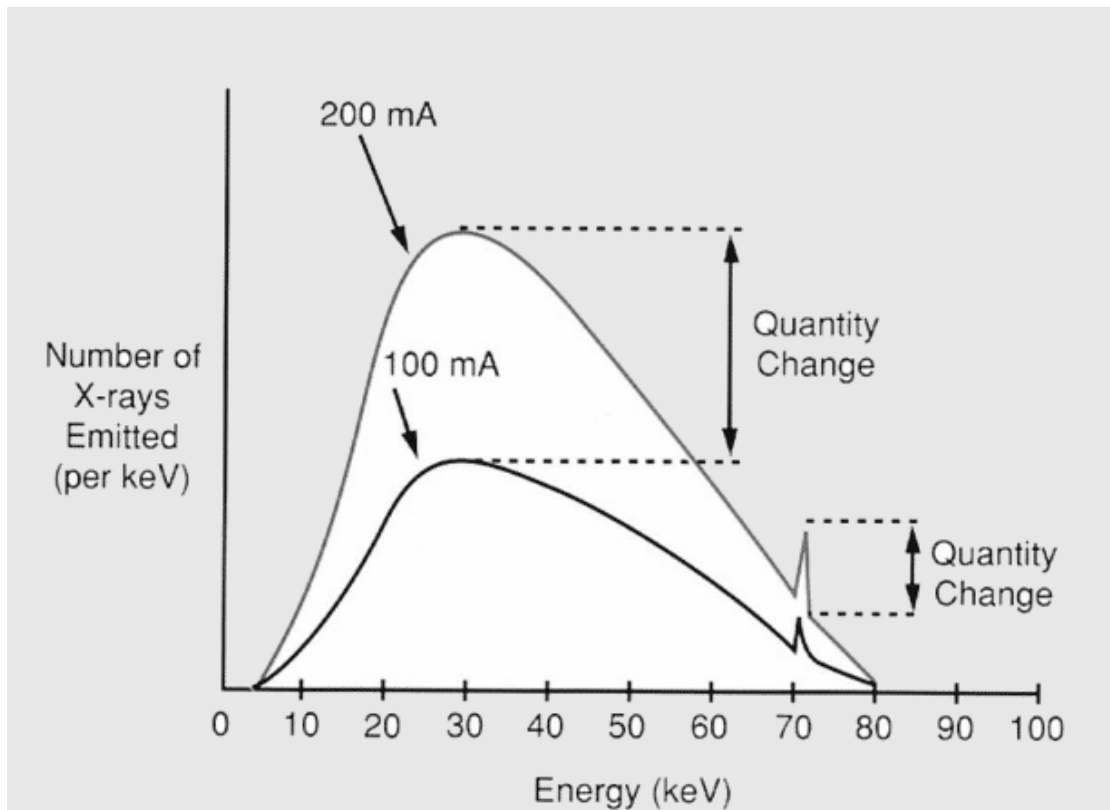


Figure A-9 Change of current leads to change of X-Ray intensity (with no spectrum change)
[9]

Appendix B: SkyScan 1076 Technical Specifications

The SkyScan 1076 is a high resolution low dose X-ray scanner for in-vivo 3D reconstruction. The application for this system is to scan small laboratory animals with detectable details up to 9 microns and has been defined as a biomedical CT Scanner. This model of the SkyScan scanner is no longer in production as of October 2010, and has been replaced with the new SkyScan 1176 model.

B.1. Equipment Limitations

Object Limitation

Maximum Object Size:	65 mm diameter by 400 mm length
Maximum Object Scan (two scans):	68 mm diameter by 200 mm length
(one scan):	35 mm diameter by 200 mm length

X-Ray Source

Continuously Variable Voltage Range:	20-100kV
Maximum Power Output:	10W
Spot Size:	<5 μm (@ 4 W measurement)
X-Ray Filters:	Al 0.5 mm, Al 1.0 mm, Ti 0.025 mm, None (all have purity greater than 99.9%)

X-Ray Detector

Detector Type:	Cooled digital X-ray camera with fibre-optic coupling to a scintillator
Resolution:	10 Mega pixel (4000x2300x12bit)
Reconstruction Array Pixel Size:	9 μm /18 μm /35 μm
Reconstruction Array Cross Section:	8000x8000 to 1000x1000 pixels (Resolution dependent)
Cross Section Format:	Isotropic Grid
Spatial resolution	
Isotropic resolution size	<9 μm voxel
Low contrast resolution	<15 μm voxel

Scanning System

System Type:	Source-detector pair rotation
Minimum Step Size Rotation:	0.02 degrees
Object Positioning Accuracy:	50 μm
Object Positioning Length:	400 mm
Camera Positioning/Alignment:	50 mm
Camera Accuracy:	1 μm
Camera Stability During Scanning:	<10 μm

B.2. Software Limitations

Reconstruction Array

Reconstruction Algorithm:	Modified Feldkamp: multislice volumetric (cone-beam)
Maximum Slice Reconstruction:	2000 (one scan)
Reconstruction Time:	1.1 second per cross section (@ 1Kx1K pixels, 0.7 degree/step, single computer)
Minimum Rotation Step Size:	0.18 degrees

Flexible to do full image, partial image reconstruction and possibility for local reconstruction with objects bigger than field of view. Recommended additional imaging is an additional 2 mm length on all sides of the object for best reconstruction results. The carbon test bed is setup for this with additional scan width compared to object size.

B.3. Setup Procedure

B.3.1 Start Up

The SkyScan micro-CT system requires that the source is aged to increase the longevity and to provide consistent X-ray spectrum output before use. This requires that whenever the system has been powered down it will need to activate the source for a period of at least 15 minutes dependent on the last use date of the equipment. No operation for a period of a month requires an aging of at least one hour before operation.

B.3.2 Sample Preparation

The sample must be within the insertion bed to avoid moving parts and taped down to avoid vibrations from movement of the scanning unit. The plane of interest in the PCB should also be as horizontal as possible in the scanning plane of the bed, as this will centralise the output model files and require less post processing. This will be unavoidable for larger samples where board warping has occurred.

Before commencing a scan, a new flat field image needs to be taken to remove highlighting of the detectors, filters and the carbon composite bed from the X-ray images. This involves the CT scanner using the X-ray source on the detectors with and without the bed to remove the inherent interference from the unit. This should be reacquired upon changing any of the configuration settings to effectively remove highlighting from each 2D X-ray image.

The SkyScan-1076 has internal and external radiation shields which have a <1 uSv/h rating on the surface whilst the X-ray source is on. The external radiation shield can be opened when an internal X-ray shutter is closed, allowing samples to be put into the SkyScan unit. The external radiation shield protects the carbon bed entry point. When the bed is within the unit the external radiation shield is locked in place.

An initial scout scan takes place upon the entry of the sample into the SkyScan unit, taking a large stitched continuous 35 µm X-ray image of the bed using the last 35 µm resolution settings used. The scout image is then used for navigation of the sample,

which starts the setup for manual movement and positioning around the sample. The manual scan is equivalent to a single 2D X-ray image but at the limitation of a single scan (35 mm by 14 mm). Manual scans are also able to be taken at an angle, which allows for finer tuning of the X-ray to the sample in the chamber.

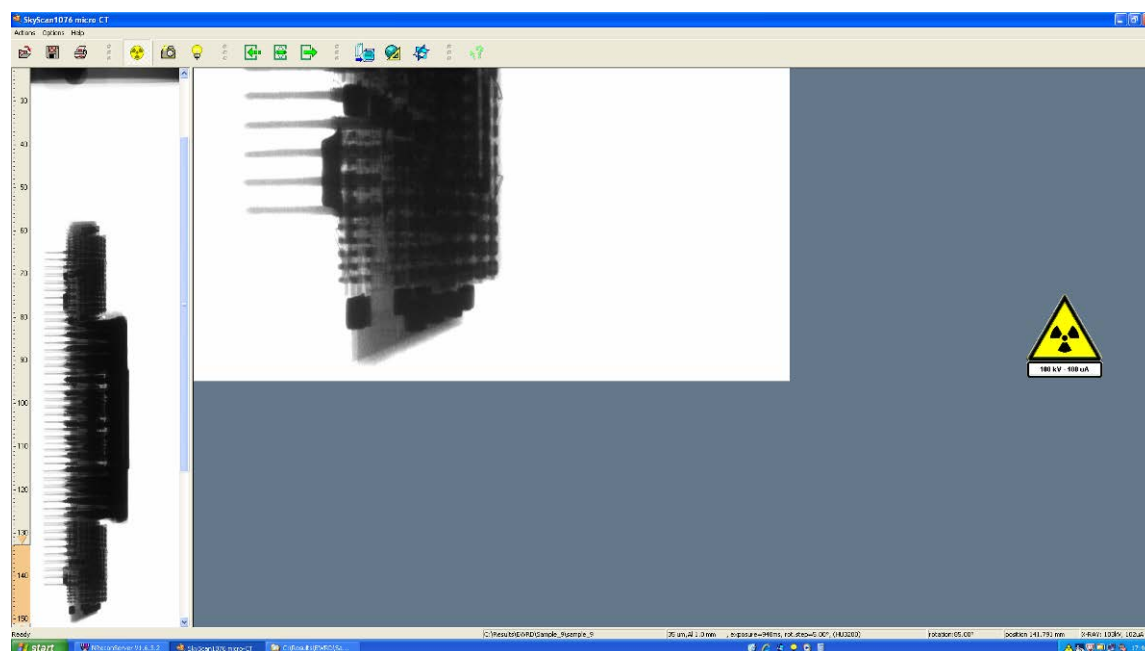


Figure B-1 Screen capture of the SkyScan 1076 interface page. On the left hand side of the image is the scout scan image. Central to the image shows a manual scan capture. Power settings can be seen underneath the radiation symbol.

B.3.3 X-ray Setup

Configuration of the X-ray source is important for getting the correct brightness and contrast to the X-ray images taken whilst performing a CT scan. The voltage and current of the X-ray source need to be tuned to the individual sample and sections of the PCB. As the source and detector set move, the X-ray has various penetration depths through the board, which affects the image retrieved from the CT scan. A manual scan was performed at zero and sixty degrees to check the X-ray penetration.

Filtering the X-ray source cleans the images produced and reduces secondary effects such as streaking around edges of the images. The 1 mm aluminium filter was used almost exclusively during the CT scanning as it removed the lower energy radiation emitted from the source.

The frame averaging of each X-ray image also needs to increase with the density of the onboard components and the number of internal layers within the PCB. This is due to the amount of metal sources generating scattering. Averaging also significantly increases the scan time as it takes multiple captures. This also removed noise from motion blur from the moving source/detector setup and vibrations of the sample.

B.3.4 Scan Setup

Once the X-ray source has been setup to match the PCB and sampled through different density areas to ensure good overall images, the scanning process can begin. The scan widths are predetermined to be either 35 mm or 68 mm, which will move the detectors to preset locations based on which scan is performed. A 68 mm scan involves two 35 mm scans on the left and right half of the PCB sample, where the extra 2 mm overlapping in the center is used for reconstruction of the image.

The length of a single scan is 14 mm, such that the collective X-ray image will be stitched together with the post processing software, Nrecon. This is a key point in determining the length of the scan time. The scan also needs to be setup with an extra 2 mm scan distance on ends of the selected sample area, as reconstruction software will not have enough data to create a full 3D image set in those regions.

The scanning software is also capable of creating batch scans using the same settings, to allow for several locations or samples to be captured automatically.

B.4. Experiment Configuration

Table B-2 Configuration and result of the data collection on the SkyScan 1076

Dataset Description	Scan Size	Filter	Voltage	Current	Exposure Time	Frame Averaging	Rotation Step Size	Resolution	Dataset Size	Scan Time
Sample 1 - Wound Inductor Coil	36.2x68mm	Al 1.0mm	100kV	100uA	474ms	2	0.7°/step	35µm	1.16 GB	00:42:24
Calibration Board	18.1x68mm	Al 1.0mm	100kV	100uA	316ms	4	0.5°/step	35µm	0.83 GB	00:35:00
Sample 2	18.1x68mm	Al 1.0mm	100kV	100uA	790ms	4	0.7°/step	35µm	0.59 GB	00:42:58
Sample 1 - DIP IC	18.1x68mm	Al 1.0mm	100 kV	100uA	474ms	4	0.7°/step	35µm	0.59 GB	00:30:28
Sample 1 - DIP IC Low Res	18.1x68mm	Al 1.0mm	100kV	100uA	474ms	4	5.0°/step	35µm	0.08 GB	00:07:21
Potted Assembly - Inductor	18.1x68mm	Al 1.0mm	100kV	100uA	948ms	4	5.0°/step	35µm	0.14 GB	00:16:26
Sample 3 - Focus PGA	36.2x68mm	Al 1.0mm	100kV	100uA	632ms	4	5.0°/step	35µm	0.18 GB	00:16:42
Sample 3 - Unfocused PGA	36.2x68mm	Al 1.0mm	100kV	100uA	316ms	4	5.0°/step	35µm	0.18 GB	00:13:27
Sample 3 - Low Power	18.1x68mm	Al 1.0mm	70kV	100uA	632ms	2	15.0°/step	35µm	0.07 GB	00:06:47
Sample 3 - Edge PGA	18.1x68mm	Al 1.0mm	100kV	100uA	2356ms	4	2.5°/step	9µm	2.68 GB	00:39:24
Sample 4	72.4x34.6mm	Al 1.0mm	100kV	100uA	3534ms	4	5.0°/step	9µm	4.77 GB	01:32:11
Sample 3 - Internal layer	18.1x68mm	Al 1.0mm	100kV	100uA	2945ms	2	0.5°/step	9µm	22.1 GB	04:04:35

B.5. Reconstruction Algorithm Comparison

For the operation of our experiment we used Nrecon on a single PC with 10 processing threads active at DSTO. A 4K x 4K cross section format was used for 9 μm resolution.

cross section format:	1K x 1K	2K x 2K	4K x 4K	8K x 8K	15K x 15K
number of cross sections:	615	1229	2255	2495	2610
number of projections:	499	996	1990	2157	8100
Single PC: rec.time (speed up)					
Nrecon, single PC	3m 58s	58m	15h 13m	59h 12m	estim: 2 months
GPUrecon, single PC with GTX590	21s (x11)	4m 7s (x14)	1h 2m (x15)	4h 35m (x13)	140h
InstaRecon, single PC	21s (x11, x1)	150s (x23, x1.6)	28m (x32, x2.2)	1h8m (x52, x4)	not possible
8xTesla GPU cluster	14s (x17, x1.5, x1.5)	98s (x38, x2.5, x1.5)	19m (x48, x3.2, x1.5)	1h8 (x52, x4, x1)	18.5h
Cluster: rec.time (speed up)					
Nrecon, 4PCs	43s	11m23s	3h0m	11h40m	estim: 2 weeks
GPUrecon, 4PCs with GTX590	12s (x3.6)	1m24s (x7.3)	24m (x7.5)	1h22m (x8.5)	estim: 45h
InstaRecon, 4PCs	18.7s (x2.3, x0.64)	114s (x5.8, x0.73)	21m (x8.5, x1.1)	51m46s (x13, x1.5)	not possible
8xTesla GPU cluster	14s (x3, x0.85, x1.3)	98s (x7, x0.8, x1.2)	19m (x9.5, x1.3, x1.1)	68m (x10, x1.2, x0.8)	18.5h

Figure B-2 Reconstruction Algorithm Comparison [4]

Appendix C: Calculations

C.1. Minimum Resolution Calculation

For a pixel to identify the density of the metal track, we need to have the source to produce a photon deficit over one detector.

From the samples used in the experiment the minimum track size was 100 μm with most tracks of 300 μm . The subsequent resolution settings used were 9 μm and 35 μm . As the metal tracks are small and next to low density material, they are subjected to partial volume effect. At worst case the outer two pixels may not contain the correct data, so they will be removed from the counted dataset for determining minimum detected pixels. Finally to not be removed from an overall data set as noise or a singularity, there should be neighbouring pixels of similar data.

100 μm width track with 9 μm scan size

$$\begin{aligned} 100 \mu\text{m} / 9 \mu\text{m} &= 11.1 \text{ pixels of data} \\ 11.1 \text{ pixels} - 2 \text{ partially filled pixels} &= 9 \text{ pixels of track data} \\ &\text{Correct sampling} \end{aligned}$$

100 μm width track with 35 μm scan size

$$\begin{aligned} 100 \mu\text{m} / 35 \mu\text{m} &= 2.8 \text{ pixels of data} \\ 2.8 \text{ pixels} - 2 \text{ partially filled pixels} &= 0.8 \text{ pixels of track data} \\ &\text{Under sampled} \end{aligned}$$

300 μm width track with 9 μm scan size

$$\begin{aligned} 300 \mu\text{m} / 9 \mu\text{m} &= 33.3 \text{ pixels of data} \\ 33.3 \text{ pixels} - 2 \text{ partially filled pixels} &= 31 \text{ pixels of track data} \\ &\text{Correct sampling} \end{aligned}$$

300 μm width track with 35 μm scan size

$$\begin{aligned} 300 \mu\text{m} / 35 \mu\text{m} &= 8.5 \text{ pixels of data} \\ 8.5 \text{ pixels} - 2 \text{ partially filled pixels} &= 6 \text{ pixels of track data} \\ &\text{Correct sampling} \end{aligned}$$

Minimum track width with 9 μm resolution

$$\begin{aligned} 3 \text{ pixels of track data} + 2 \text{ worst case partially filled pixels} &= 5 \text{ pixels of data} \\ 5 \text{ pixels} \times 9 \mu\text{m} &= 45 \mu\text{m track width} \end{aligned}$$

C.2. Estimated PCB Data Size and Time Requirement

Most of the scanned volumes for our experiment were limited to smaller areas of interest which were 68 mm by 32 mm (Appendix B.4). However, it may not be obvious where a fault on the PCB exists requiring the entire board to be scanned. A benchmark for typical PCB sizes of 250 mm by 100 mm will be used to determine the system requirements. For this extrapolation we will assume that the track width is

the finest feature that needs to be resolved. The following section will use the SkyScan 1076 results and parameters from the experiments where necessary.

The maximum size object that we want to be able to scan is:
 $250 \text{ mm} \times 100 \text{ mm} = 25,000 \text{ mm}^2$

The scan sizes used during the experiment are:
 $36.2 \text{ mm} \times 68 \text{ mm} = 2461.6 \text{ mm}^2$
 $72.4 \text{ mm} \times 34.6 \text{ mm} = 2505.0 \text{ mm}^2$

For a standard PCB with less complex board design and track routing, a typical track width of $300 \mu\text{m}$ can be assumed to be used. Using the preset $35 \mu\text{m}$ scan resolution, the track will have a resolvable detail of 6 pixels in width. This would be enough detail to resolve the most defects as stated in Section 2.3.2. The outcome of this would result in an approximate raw dataset of 18GB and require 210-260 hours to scan dependent on material density (Calculation below).

From here we are able to use the size and time to forward estimate the time taken for an entire scan. Using Sample 3 - Focus PGA and Unfocused PGA (Appendix B.4) scan time and memory resolution settings at $35 \mu\text{m}$

- Scan area size increase from 2461.6 mm^2 to $25,000 \text{ mm}^2$ is an increase of 10 times more memory usage per image and time (a larger detector from a larger CT unit will increase the cross sectional area taken and reduce the scan time)
- Angular resolution increasing from $5.0^\circ/\text{step}$ to $0.5^\circ/\text{step}$ is an increase of 10 times samples which will affect the memory and scan time
- To finely tune the contrast of the system, the current and voltage settings has the finer adjustment ability in comparison to exposure time, and would need to be increased slightly for adjustment. This would increase the time taken by 1.2 times but may be reduced with different filters and higher power levels.
- Higher frame averaging would also be needed for improvements for signal to noise ratio. Increasing to 8 frames of averaging will affect the time taken to scan and increase pre-processing time but would ideally not increase the memory requirements (frames averaged then stored)

Summary for adjustment for Sample 3 Low Resolution

Area size increase:	Memory x10,	Time x10
Angular Resolution:	Memory x10,	Time x10
Sampling:		Time x2
Contrast:		Time x1.2

Dataset size $0.18 \text{ GB} \times 10 \times 10$	= 18 GB
Scan Time: $(13-16) \text{ mins} \times 10 \times 10 \times 1.2 \times 8$	= (208 - 256) hrs

A more complex PCB with smaller track widths down to $100 \mu\text{m}$ (equivalent to sample 3's internal track size) would require a $9 \mu\text{m}$ resolution scan to give 9 pixels of data. The resultant outcome of this system would yield a raw unprocessed dataset of 884-954 GB and a scan time of 720-768 hrs for a normal density PCB (Calculation below).

For estimating a high resolution scan outcome, the results of Sample 3 - Internal layer and Sample 4 (Appendix B.4) were used. Both time and memory resolution settings at 9 μm and making the same adjustments as listed above where necessary, with the addition of

- The change in Sample 4 scan area size from 2505.0 mm^2 to 25000 mm^2 is an increase of memory by 5 times and a decrease in of time by 2 times.
- The change in Sample 3 - Internal layer scan area size is from 1230.8 mm^2 to 25000 mm^2 is an increase of memory by 20 times and double the time.
- Sample 3 - Internal layer needs to be increased to a full raw construction set, where a half reconstruction set and only had images over 180°. This requires a memory and time adjustment of 2.

Summary for adjustment for Sample 4

Area size increase:	Memory x10,	Time x10
Angular Resolution:	Memory x10,	Time x10
Sampling:		Time x2
Contrast:		Time x1.2

Dataset size: 4.77 GB x 10 x 10 x 2 = 954 GB

Scan Time: 1.5 hr x 10 x 10 x 2 x 2 x 1.2 = 720 hr

Summary for adjustment for Sample 3 - Internal layer

Area size increase:	Memory x20,	Time x20
Angular Resolution:	None	
Angular Sweep Range:	Memory x2,	Time x2
Sampling:		Time x4
Contrast:		Time x1.2

Dataset size: 22.1 GB x 20 x 2 = 884 GB

Scan Time: 4 hr x 20 x 2 x 4 x 1.2 = 768 hr

Appendix D: Image Colour Contrast Scales

For the contrast scale provided with the 16-bit TIFF file the data range for each pixel is between 0 - 65535 on the colour slide. Below are the standard colour scales used.

D.1. Grey Colour Scale

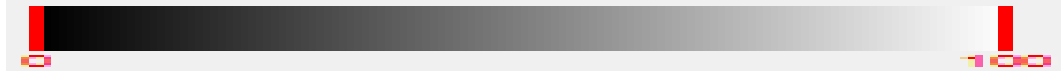


Figure D-1 Grey Colour Scale

D.2. Dynamic Colour Scale 1



Figure D-2 Colour Bar Style 1

D.3. Dynamic Colour Scale 2



Figure D-3 Colour Bar Style 2

DEFENCE SCIENCE AND TECHNOLOGY ORGANISATION DOCUMENT CONTROL DATA							
				1. PRIVACY MARKING/CAVEAT (OF DOCUMENT)			
2. TITLE Analysis of Multilayered Printed Circuit Boards using Computed Tomography				3. SECURITY CLASSIFICATION (FOR UNCLASSIFIED REPORTS THAT ARE LIMITED RELEASE USE (L) NEXT TO DOCUMENT CLASSIFICATION) Document (U) Title (U) Abstract (U)			
4. AUTHOR(S) Samuel Fox, Greg Perry				5. CORPORATE AUTHOR DSTO Defence Science and Technology Organisation PO Box 1500 Edinburgh South Australia 5111 Australia			
6a. DSTO NUMBER DSTO-TR-2973		6b. AR NUMBER AR-015-962		6c. TYPE OF REPORT Technical Report		7. DOCUMENT DATE May 2014	
8. FILE NUMBER 2013/1117926/1	9. TASK NUMBER 07/308	10. TASK SPONSOR DGJFI		11. NO. OF PAGES 36		12. NO. OF REFERENCES 9	
DSTO Publications Repository http://dspace.dsto.defence.gov.au/dspace/				14. RELEASE AUTHORITY Chief, Cyber and Electronic Warfare Division			
15. SECONDARY RELEASE STATEMENT OF THIS DOCUMENT <i>Approved for public release</i>							
OVERSEAS ENQUIRIES OUTSIDE STATED LIMITATIONS SHOULD BE REFERRED THROUGH DOCUMENT EXCHANGE, PO BOX 1500, EDINBURGH, SA 5111							
16. DELIBERATE ANNOUNCEMENT No Limitations							
17. CITATION IN OTHER DOCUMENTS Yes							
18. DSTO RESEARCH LIBRARY THESAURUS Inspection, Tomography, Electronics							
19. ABSTRACT Computed Tomography is a technique that can be performed using a set of X-ray images to re-create a three dimensional dataset which contains information about internal structure. Analysis of multilayered Printed Circuit Boards with their components using this technique allows for the non destructive evaluation of internal layers of failed boards. This report presents the results of computerised tomography on multilayered Printed Circuit Boards using a SkyScan 1076.							